



# **Particle Emissions from a Euro 5a Certified Diesel Passenger Car**

**A. Mamakos, C. Dardiotis, A. Marotta, G. Martini,  
U. Manfredi, R. Colombo, M. Sculati, P. Le Lijour, G. Lanappe**

EUR 24855 EN - 2011

The mission of the JRC-IE is to provide support to Community policies related to both nuclear and non-nuclear energy in order to ensure sustainable, secure and efficient energy production, distribution and use.

European Commission  
Joint Research Centre  
Institute for Energy

**Contact information**

Giorgio Martini  
Address: Joint Research Center, Via Enrico Fermi 2749, 21027 Ispra (VA), Italy  
E-mail: [giorgio.martini@jrc.ec.europa.eu](mailto:giorgio.martini@jrc.ec.europa.eu)  
Tel.: +39 0332 789293

<http://ie.jrc.ec.europa.eu/>  
<http://www.jrc.ec.europa.eu/>

**Legal Notice**

Neither the European Commission nor any person acting on behalf of the Commission is responsible for the use which might be made of this publication.

***Europe Direct is a service to help you find answers  
to your questions about the European Union***

**Freephone number (\*):  
00 800 6 7 8 9 10 11**

(\*): Certain mobile telephone operators do not allow access to 00 800 numbers or these calls may be billed.

A great deal of additional information on the European Union is available on the Internet.  
It can be accessed through the Europa server <http://europa.eu/>

JRC 65206

EUR 24855 EN  
ISBN 978-92-79-20486-9  
ISSN 1831-9424  
doi:10.2788/3173

Luxembourg: Publications Office of the European Union

© European Union, 2011

Reproduction is authorised provided the source is acknowledged

*Printed in Italy*

## TABLE OF CONTENTS

1	INTRODUCTION .....	3
2	EXPERIMENTAL .....	5
2.1	Vehicle .....	5
2.2	Fuel and Lube oil .....	5
2.3	Test Cycles .....	5
2.4	Sampling systems and conditions .....	7
2.4.1	PM sampling.....	8
2.4.2	Particle number sampling.....	8
2.5	GASEOUS POLLUTANTS .....	10
3	Results .....	11
3.1	Temperature profiles.....	11
3.2	PM emissions.....	14
3.3	PN emissions .....	17
3.3.1	Real time traces .....	17
3.3.2	Effect of DPF soot load .....	18
3.3.3	Emissions during regeneration.....	21
3.3.4	Sub 23 nm particles.....	23
4	Conclusions .....	28
5	LIST OF SPECIAL TERMS AND ABBREVIATIONS .....	30
6	REFERENCES .....	31

# 1 INTRODUCTION

Diesel Particulate Filters (DPF) have become an indispensable component of diesel light duty exhaust aftertreatment systems, following the introduction of a particle number standard at Euro 5 stage. The operation principle of DPF systems is based on the separation of the airborne particles from the gas stream by deposition on a collecting surface. As soot accumulates onto the DPF there is a need for a periodic regeneration (i.e. consumption of the accumulated soot) in order to avoid clogging of the DPF or uncontrolled oxidation of the soot that can potentially damage the DPF. Combustion of soot with oxygen occurs at a temperature of about 650°C which is rarely achieved in the exhaust of the diesel vehicles. The combustion temperature can be reduced however through the use of a catalyst, by means of either coating the DPF walls or directly adding it in the fuel. Alternatively or in addition, the oxidation rate of soot can be increased, and therefore the regeneration temperature can be decreased, by production of Nitrogen Dioxide (NO<sub>2</sub>) which is a more active oxidant than oxygen.

Under certain operating conditions, the exhaust gas temperature can exceed the temperature required for the oxidation of the accumulated soot, that depends on the aftertreatment configuration employed and the soot loading of the DPF, at which point regeneration of the DPF occurs. This type of regeneration is referred to as passive regeneration since it occurs naturally without requiring any kind of interference from the Emissions Control System (ECS). In practise however, the exhaust gas temperature is too low to sustain regeneration of the DPF under all operating conditions.

In order to ensure that the DPF will regenerate regularly and, most importantly, avoid excessive soot accumulation and stochastic regeneration, the ECS continuously monitors the pressure drop across the DPF which is indicative of soot loading. If deemed necessary, the ECS can also trigger regeneration (active regeneration) in order to increase the exhaust gas temperature to levels that would initiate and sustain regeneration. This is achieved by means of generating an exotherm through delayed fuel injection in the cylinder or even a post-injection of fuel in the exhaust manifold in order to increase the exhaust gas temperature to levels that would initiate and sustain regeneration. Additional or complementary engine measures to trigger regeneration include Exhaust Gas Recirculation (EGR) shut-off and throttling of the exhaust.

In most cases a Diesel Oxidation Catalyst (DOC) is employed upstream of the DPF, which has double role during regeneration: On one hand it oxidizes some of the Nitrogen Monoxide (NO) mainly produced in the engine, to Nitrogen Dioxide (NO<sub>2</sub>). NO<sub>2</sub> allows soot oxidation at much lower temperatures (280-370°C) than oxygen, thus enhances passive regeneration. The DOC plays also a very important role in active regeneration, producing the exotherm needed to sustain soot regeneration, through oxidation of late injected or post injected fuel.

A side effect of DPF regeneration is the increased emission of gaseous pollutants and particulate matter. The contribution of such elevated emissions occurring during regeneration events to the total emitted quantity of pollutants during the lifetime of the vehicle will depend on the frequency of such regeneration events. Accordingly, the European regulations classify the regenerating aftertreatment devices (including DPF systems) to continuous or periodic depending on whether the regeneration occurs in each repetition of the legislated test cycle or not. Vehicles equipped with continuously regenerating DPF systems do not require a special test procedure. On the other hand, vehicles equipped with DPF systems that regenerate on a periodic basis need to be tested under both conditions (i.e. with and without regeneration events occurring over the test cycle) and the emission levels are determined by

means of weighting the two different emission levels according to the frequency of regeneration events. Currently the procedure applies only to gaseous pollutants and Particulate Matter (PM) but not for the recently introduced particle number emissions.

There is limited information available in the literature on the particle number emissions during regeneration of DPF systems employed in light duty vehicles [1, 2, 3, 4, 5, 6, 7, 8, 9, 10]. The situation is further complicated by the fact that different experimental setups were employed in the different studies, thus hindering a direct comparison of the results. A survey of the available data [11] suggested that particles emitted during regeneration are volatile in nature having a size peaking at around 10 nm. As such, they were not expected to contribute to the regulated “non-volatile” particle number emissions. The latter are defined as thermally treated particles counted by a Condensation Particle Counter (CPC) having a 50% detection efficiency at 23 nm [12]. The requirements set by the regulations on the thermal treatment include hot dilution of at least 10:1 and 150°C, followed by heating and reduction of partial pressures of the volatile material, sufficient to achieve a higher than 99% vaporisation of 30 nm tetracontane particles at inlet concentrations of at least 10000 #/cm<sup>3</sup>. In line with the recommendations laid down in the regulations, most commercial systems (commonly referred to as PMP systems after the Particle Measurement Programme that recommended the particular measurement approach) employ an Evaporation Tube (ET) heated at a wall temperature of 300 to 400°C, downstream of the primary diluter, followed by a secondary diluter capable of maintaining a dilution ratio of at least 10, using conditioned air at ambient temperatures.

Some recent study [13] showed that in the presence of sulphates, some pyrolysis or charring of organic vapours may occur in thermodenuders, with the authors speculating that similar effects can also occur in evaporating tubes of commercial PMP systems. The reduction of sulphur content in European diesel fuels to less than 10 ppm [14] has effectively reduced sulphate emissions under normal operation. However, increased sulphate emissions have been reported during regeneration [4], which were attributed to storage of sulphur compounds (originating either from the fuel or from the lubrication oil) in the DPF and subsequent release during regeneration. It is therefore suspected that such pyrolysis of volatile material, resulting in artificial “non-volatile” particle formation inside the ET, might be an issue during DPF regeneration.

One additional shortcoming of the aforementioned studies was that they investigated the emission performance of first generation of DPF-equipped vehicles or even prototype DPF systems. It is not clear whether the results of these investigations are also valid for late technology DPF-equipped diesel vehicles. The present study investigated the particle emission performance of a late technology, Euro 5 certified diesel passenger car equipped with a DPF. The study addressed both the effect of soot loading and DPF regeneration on particle emissions.

## 2 EXPERIMENTAL

### 2.1 VEHICLE

The vehicle tested in this study was a turbocharged, 1.25 l, Euro 5 compliant diesel passenger car, with a rated power at 55 kW. It was obtained from a rental company and had an accumulated mileage of 6402 km before testing. The vehicle was equipped with a belt-alternator starter, which was however deactivated during the measurement campaign. The vehicle was also equipped with DPF close coupled to the engine, and installed downstream of an oxidation catalyst. No information is available on the DPF substrate material, porosity and (if any) catalytic washcoat. Periodic regeneration of the DPF was achieved by means of fuel post-injection and EGR-shut off, capable to raise the temperature upstream of the DPF above 600°C. Two thermocouples, installed upstream and downstream of the DPF, provided the means to monitor in real time the temperature of the exhaust entering and leaving the DPF. The Electronic Control Unit (ECU) signal was also recorded in real time, providing some information on the Exhaust Gas Recirculation (EGR) valve positioning.

### 2.2 FUEL AND LUBE OIL

The vehicle was tested with the originally employed lubrication oil and commercial diesel fuel, complying with Annexes 3 and 4 of Directive 2009/30/EC (sulphur content lower than 10 ppm) [14].

### 2.3 TEST CYCLES

The vehicle was tested under the standard New European Driving Cycle (NEDC) and the Common Artemis Driving Cycles (CADC) developed in the framework of the EU Artemis project [15]. The NEDC cycle, illustrated in Figure 1, been used in Europe for certification of light-duty vehicles since 2000 and consists of the urban part, commonly referred to as ECE, which includes four repetitions of the ECE15 elementary cycle, and the extra-urban part (EUDC).

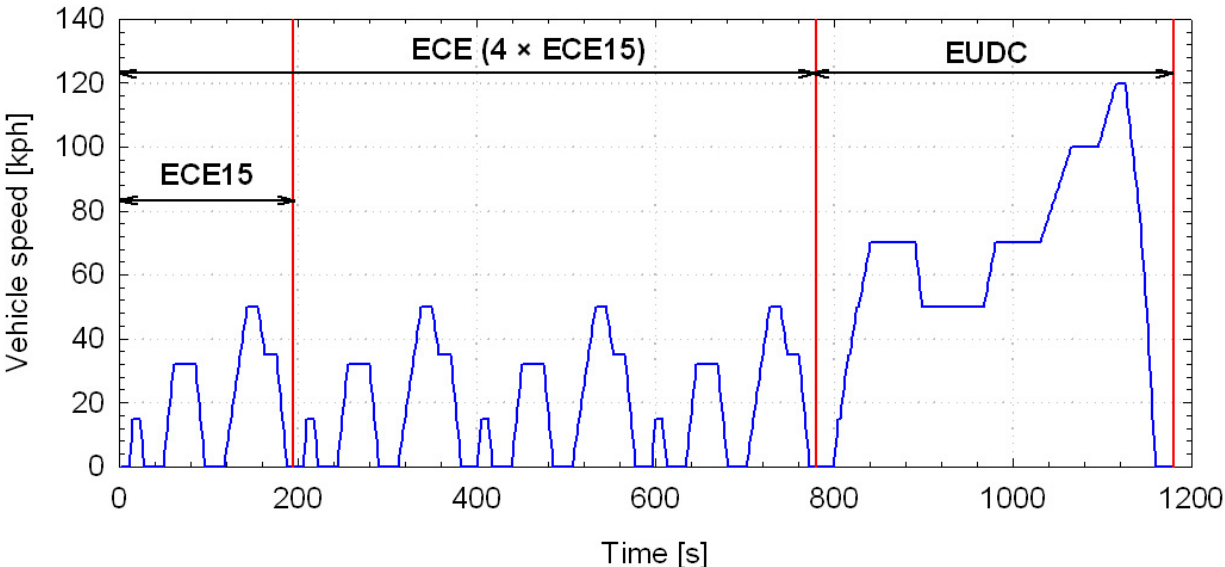


Figure 1: New European Driving Cycle (NEDC) and its two phases: Urban (ECE) and Extra-Urban (EUDC).

The Common Artemis Driving Cycle, shown in Figure 2, was developed by statistical analysis of speed profile databases from 90000 km accumulated from on-board monitoring of 80 passenger cars in France, Germany, Great Britain and Greece, supplemented by another 10000 km obtained in Switzerland and Italy under controlled traffic conditions. The CADC cycle consists of three parts representative of typical urban, rural and motorway driving conditions in Europe. The cycle also includes some warm-up and cool-down phases which are not considered in the emission characterization.

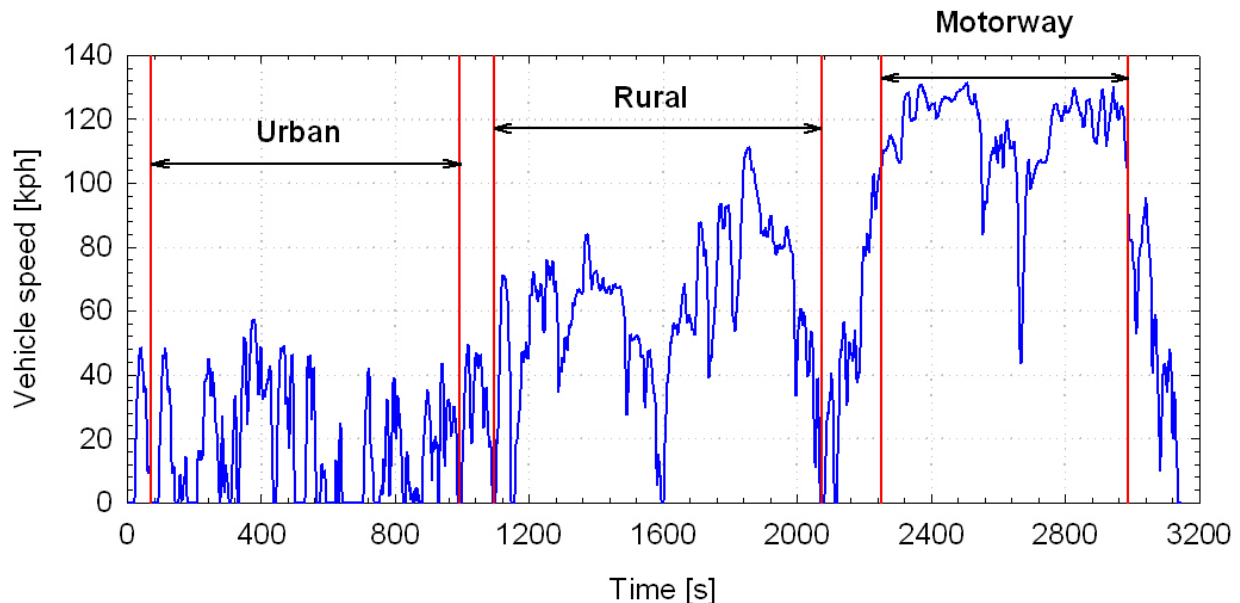


Figure 2: Common Artemis Driving Cycle (CADC) and the three PM sampling periods corresponding to Urban, Rural and Motorway driving conditions.

The vehicle was tested under both cold start and hot start NEDC. In order to ensure repeatable test conditions, three consecutive EUDC tests were performed before the CADC and the hot start NEDC tests. Cold start NEDCs were performed after soaking the vehicle overnight for more than 12 hours. In some tests, an additional load of up to 600 W, was applied externally through a configuration of 6 lamps, of 100 W each. Some measurements were also performed at a test cell temperature of  $-7^{\circ}\text{C}$ . For these tests the dynamometer settings were adjusted for a 10% decrease of the coast-down time, resulting in a corresponding increase of the resistance to progress, in accordance to the UN-ECE Regulation 83 Revision 4 [12]. The actual test matrix is summarised in Table 1.

Table 1: Number of repetitions performed for each combination of test cycle, test cell temperatures and external power consumption, examined.

	External power consumption [W]				
Cycle	0	200	300	400	600
22°C					
NEDC	3		2		2
CADC	5				2
NEDC hot	2	2		2	2
-7°C					
NEDC	4*				
CADC	2				
NEDC hot	1				

\* In one NEDC repetition the vehicle was soaked at -2°C due to a failure of the temperature conditioning system.

## 2.4 SAMPLING SYSTEMS AND CONDITIONS

Sampling was conducted according to the current legislation. The tests were carried out on a 48" 4x4 dynamometer MAHA SN 87 (roller diameter of 1.22 m and 150 kW) at the Vehicle Emissions Laboratory (VELA) of the Joint Research Centre (JRC).

In accordance to the regulations, the exhaust gas was primarily diluted and conditioned following the Constant Volume Sampler (CVS) procedure. Highly efficient dilution air filters for particles and hydrocarbons that reduce particle contributions from the dilution air to near zero were used (99.99%) of reduction of particles with size diameter of 0.3 µm).

The vehicles were coupled to the CVS transfer line by a metal-to-metal join during testing to avoid the possibility of exhaust contamination by the high-temperature breakdown of elastomer coupling elements. The exhaust was transported to the tunnel through a 5.5 m long insulated corrugated stainless steel tube. It was introduced along the tunnel axis, near an orifice plate that ensured rapid mixing with the dilution air. The flow rate of diluted exhaust gas through the tunnel was controlled by a critical orifice venture. A flow rate of 6 m<sup>3</sup>/min at standard reference conditions (20°C and 1 bar) was used for the NEDC and EUDC tests. CADC tests were performed at either 6 m<sup>3</sup>/min or 9 m<sup>3</sup>/min. The tunnel operated in the turbulent flow regime (Re>27000) with the residence time of the exhaust in the dilution tunnel being 2.6 s and 1.7 s at CVS flowrates of 6 m<sup>3</sup>/min and 9 m<sup>3</sup>/min, respectively.

A schematic of the set up is shown in Figure 3. Three different probes, placed at the same cross-section of the tunnel and facing upstream the flow, were used for sampling. One probe was used for PM measurements and the other two for particle number. These probes were installed 10 tunnel diameters downstream of the mixing point to ensure complete mixing of the dilution air and the exhaust gas.



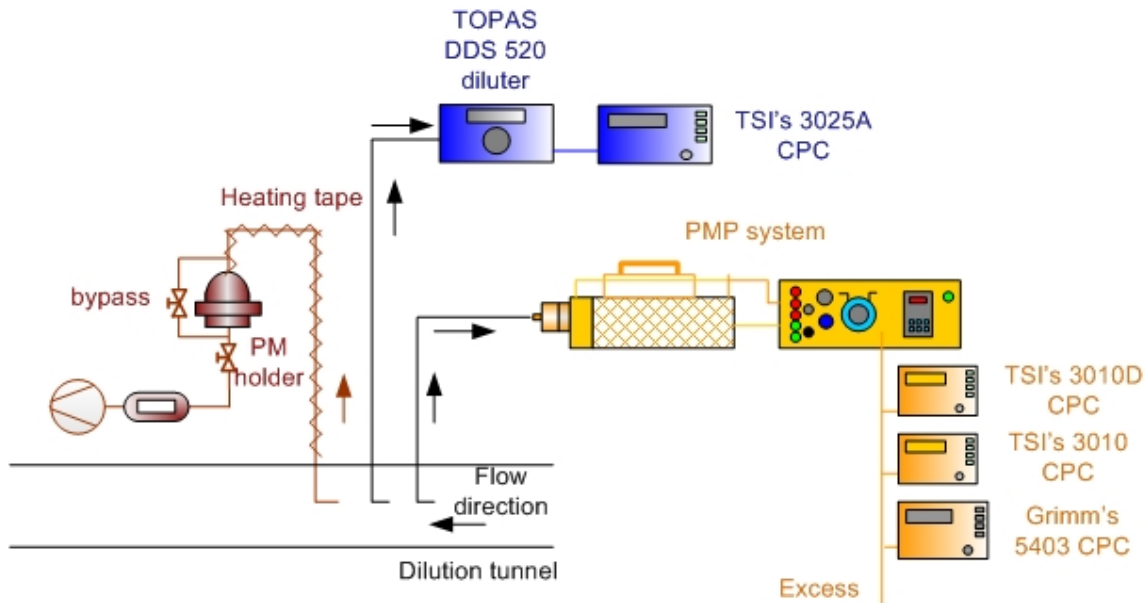


Figure 3: Experimental setup

### 2.4.1 PM sampling

PM mass was measured according to the current legislation. PM samples were drawn directly from the CVS at a constant flowrate of 50 lpm at normal conditions (0°C and 1 bar) for all the measurements to improve repeatability.

The filter holder and transfer tubing were externally heated by direct surface heating to permit aerosol stabilization of >0.2 s prior to sampling and to ensure close control of the filter face temperature to 47°C (±5°C).

PM samples were collected on 47 mm Teflon-coated glass-fiber Pallflex® TX40H120-WW filters. One single filter was employed over the entire cycle (cold start NEDC or CADC). In two particular tests however, (a cold start NEDC at -2°C and a CADC at 22°C) a back up-filter was employed in order to get some information on the contribution of adsorbed material on the filters. At the end of the measurement campaign, two blank tests (one CADC and one NEDC) were also performed to determine the background PM in the CVS tunnel (CVS running with the transfer hose plugged), using two TX40 filters in series.

The filters were kept in a control temperature and humidity chamber (22±1°C and 50±5% respectively), and they were weighted with a Mettler Toledo model UMX2 balance (sensitivity 10<sup>-7</sup> g) before and after the measurement, allowing at least two hours for conditioning. Electrostatic charge effects were minimized by the use of HAUG Type EN SL LC 017782100 neutralizer and grounded conductive surfaces. Each filter was weighted two times, and the average of the weightings was used in calculating mass changes.

### 2.4.2 Particle number sampling

Aerosol samples for the particle number characterization were drawn from the CVS tunnel using a Matter Aerosol's Solid Particle Counter. This consists of an MD19-2E rotating disk diluter (Matter Aerosol AG) [16, 17, 18] for primary dilution, followed by an evaporating tube

and a secondary simple air mixer diluter. The primary diluter and the primary dilution air were heated at 150°C while the wall temperature of the evaporating tube was set at 350°C ( $\pm 1^\circ\text{C}$ ).

In order to investigate whether re-nucleation of volatile material may have occurred downstream of the ET, tests were performed at three different dilution ratios. Since the rate of nucleation exhibits a highly non-linear dependence on the saturation ratio (Kelvin effect), it is expected that the concentration of any nucleation mode particles will decrease with increasing dilution ratio. The Particle Concentration Reduction Factors (PCRF) employed in the study, were 300, 520 and 2100.

The PMP system was originally equipped with a TSI's 3790 CPC having a 50% detection efficiency at 23 nm. The particular CPC was only employed in the first two days of the measurement campaign, since it was observed that it could not maintain the condenser temperature due to some malfunctioning of the cooling system. It was subsequently replaced with a TSI's 3010D CPC also having a 50% detection efficiency at 23 nm. A TSI's 3010 CPC and a Grimm 5403 CPC having nominal 50% detection efficiencies at 10 nm and 4.5 nm, respectively, were also employed sampling in parallel downstream of the PMP system.

A TSI's 3025A CPC having a 50% detection efficiency at 3.5 nm was also employed in the study sampling from the CVS tunnel through a TOPAS DDS 520 diluter. The 3025A CPC operated at high flow mode (1.5 lpm) and the diluter was set at a dilution ratio of 100:1. The particular CPC was only employed to identify conditions of high volatile particle formation, e.g. during DPF regeneration. It was not possible however to quantify the absolute emission levels during such events since the instrument got saturated even at the highest allowable dilution ratio of the TOPAS diluter (500:1).

The CPCs were calibrated against an Ioner's EL-5030 electrometer at the end of the measurement campaign in order to determine their slope in accordance to the regulations. Poly-alpha olefin particles were employed produced in a home-made generator operating on the evaporation-condensation technique. Monodisperse particles of 100 nm mobility diameter were produced in a Tandem Differential Mobility Analyzer (T-DMA) system consisting of a Grimm's 5.5-900 DMA operating at sheath over sample flowrates of 3 lpm / 0.75 lpm followed by a TSI's 3080 LDMA operating at a sheath over sample flowrate of 10 lpm / 0.75 lpm. The produced monodisperse aerosol was mixed with make-up conditioned air in a 2 m long silicon tube (internal diameter of 6 mm). The diluted sample was subsequently split into two branches through a Y-type connector that allowed for parallel sampling with the electrometer and the CPC under evaluation, using conductive silicon tube of equal length (~15 cm). The electrometer operated at the same flowrate with the CPC under calibration (1.5 lpm in the case of the TSI's 3025A and Grimm's 5403 CPCs, and 1 lpm in the case of the TSI's 3010 and 3010D CPCs). A dilution bridge, installed upstream of the T-DMA, provided the means to control the concentrations. The experimentally determined slopes (at 5 concentration levels from 2000 #/cm<sup>3</sup> to 10000 #/cm<sup>3</sup>) are summarized in Table 2.

Table 2: Experimentally determined sloped of the four CPCs employed in the study.

CPC model	Slope
TSI's 3010	0.92
TSI's 3010D	0.87
TSI's 3025A	1.00
Grimm's 5403	0.96

## **2.5 GASEOUS POLLUTANTS**

A Horiba OVN-723A oven type (heated) analyzer was employed for the real time measurement of Nitrogen Oxides (NO<sub>x</sub>) and Total HydroCarbon (HC) emissions. Oxygen (O<sub>2</sub>), Carbon Monoxide (CO) and Carbon Dioxide (CO<sub>2</sub>) emissions were measured in real time using a Horiba MEXA-7400HTR-LE analyzer. The Horiba MEXA-7400HTR-LE analyzer was also employed to measure bag emissions in accordance to the current UN Regulation 83 [12].

### 3 RESULTS

#### 3.1 TEMPERATURE PROFILES

The recorded exhaust gas temperatures upstream of the DPF over cold start NEDC tests at 22°C and -7°C test cell temperatures are shown in Figure 4. The temperature did not exceed 230°C over the urban part of the NEDC and peaked at 400°C over the short period (~10 s) of 120 kph driving. The exhaust gas temperatures in the tests conducted at -7°C test cell temperature were approximately 20% lower.

The corresponding exhaust temperature profiles over the CADC test are shown in Figure 5. The temperatures peaked at 230°C and 360°C over the urban and rural part of the cycle. Under non-regenerative conditions, the exhaust temperature peaked at 420°C over CADC motorway. When active regeneration took place, the temperature was raised up to 700°C. During these active regeneration events, which lasted approximately 10 min, the EGR was shut-off to assist the temperature raise (Figure 6).

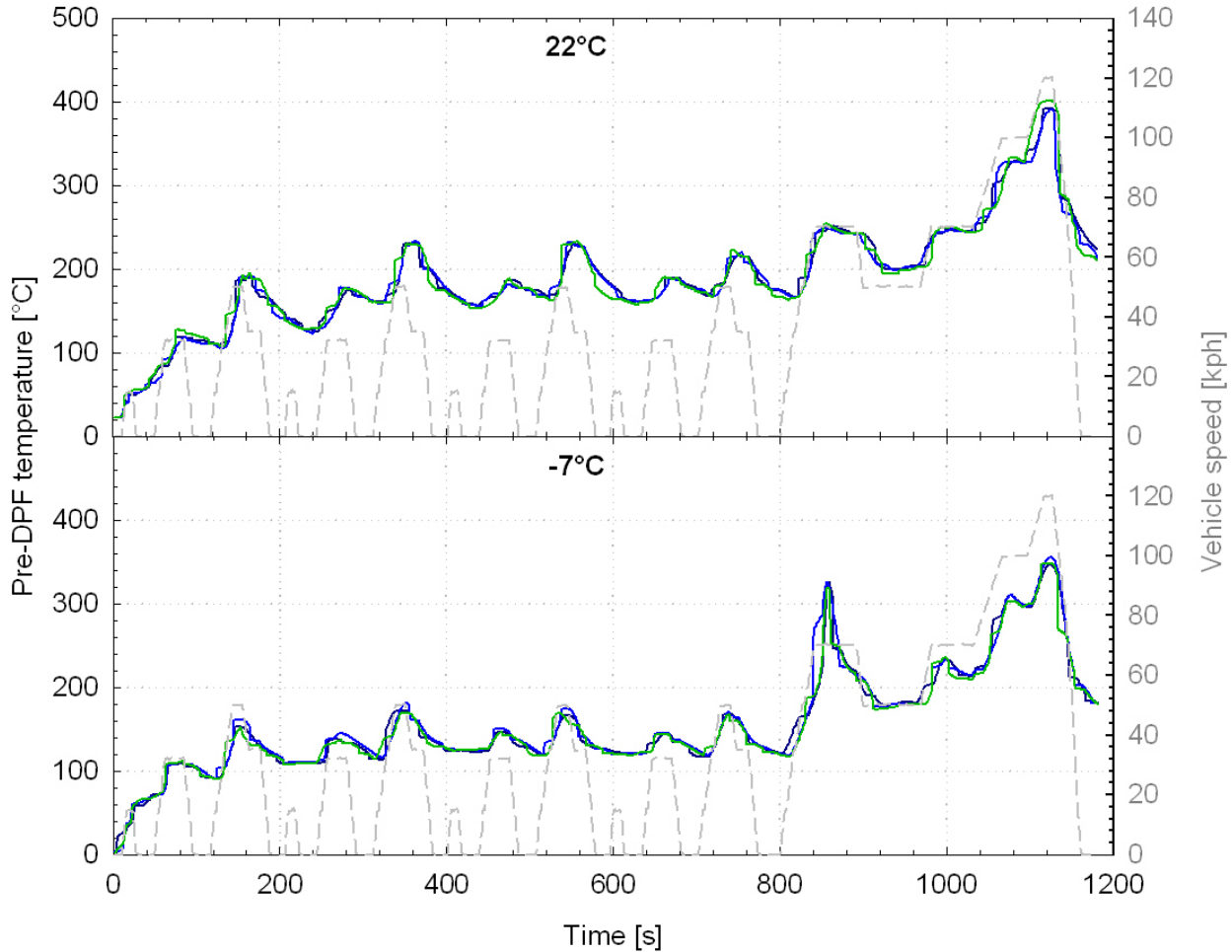


Figure 4: Exhaust gas temperatures upstream of the DPF over cold start NEDC at 22°C (upper panel) and -7°C (lower panel) test cell temperatures.

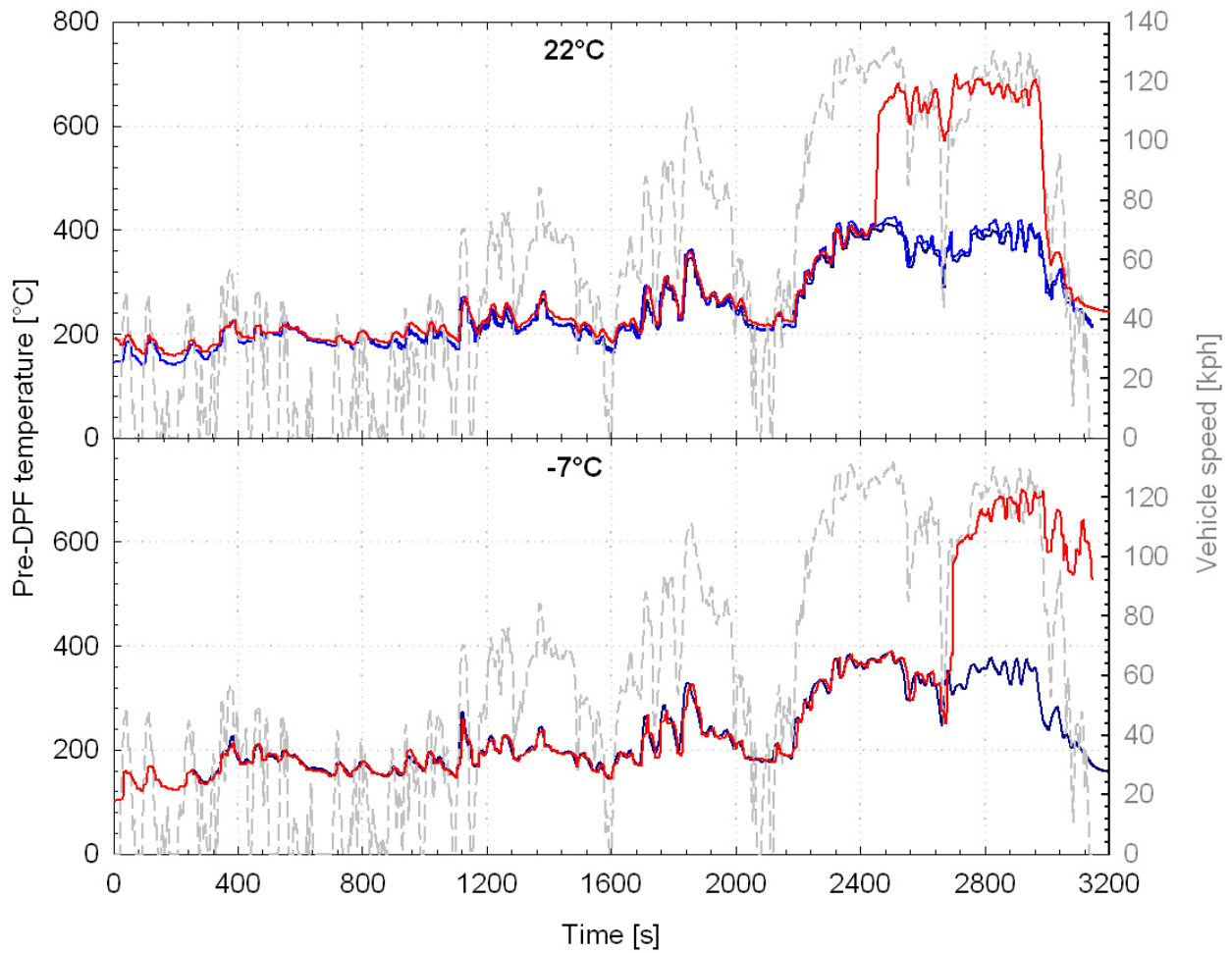


Figure 5: Exhaust gas temperatures upstream of the DPF over CADC at 22°C (upper panel) and -7°C (lower panel) test cell temperatures, under non-regenerative (blue curves) and regenerative (red curves) conditions.

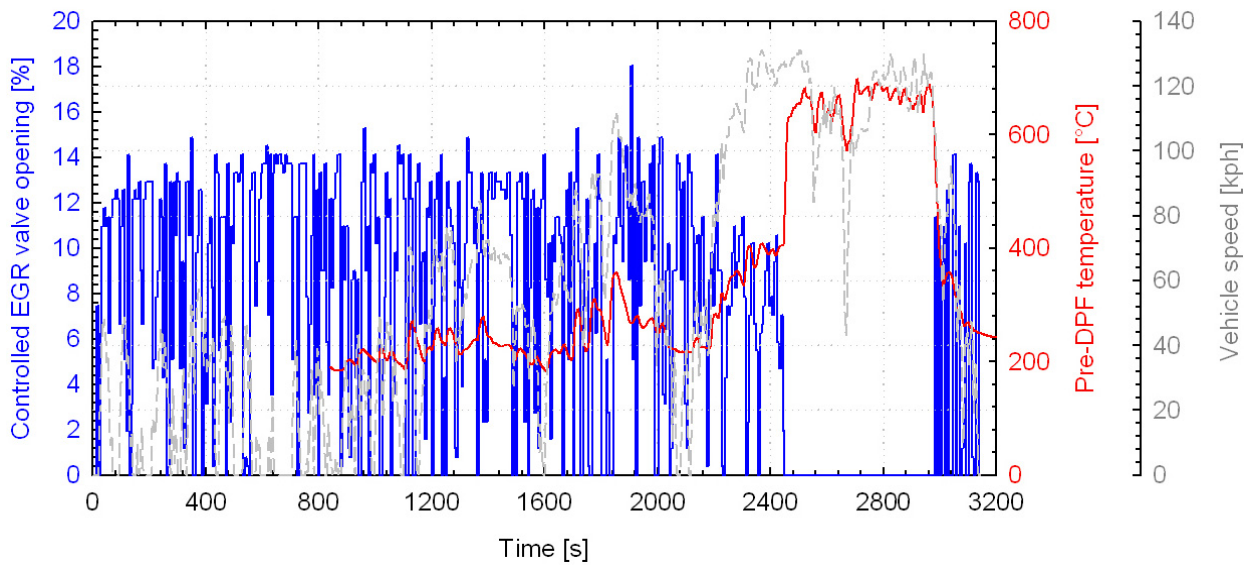


Figure 6: ECU signal (blue curve) on the EGR valve opening during a regenerating CADC test.

One concern, pertaining to the regeneration of DPF systems is the temperature increase in the CVS tunnel and most importantly the PM filter. Figure 7 shows the traces of these temperatures for two CADC tests where regeneration took place. In the test at -7°C test cell temperature, the CVS flowrate was set at 6 m<sup>3</sup>/min resulting in a peak temperature, measured downstream of the PM sampling point, of 100°C during the motorway part of the cycle. The maximum temperature at the PM filter holder was 63.5°C. The second test, shown at the lower panel of Figure 7, was performed at an ambient test cell temperature of -7°C with the CVS flow set at 9 m<sup>3</sup>/min. Due to the lower exhaust temperatures and the higher dilutions employed, the maximum temperatures in the CVS tunnel and the PM filter holder dropped to 76°C and 60.5°C, respectively. The results suggest that the 192°C threshold specified in the regulations [12] for regenerative conditions is unrealistically high.

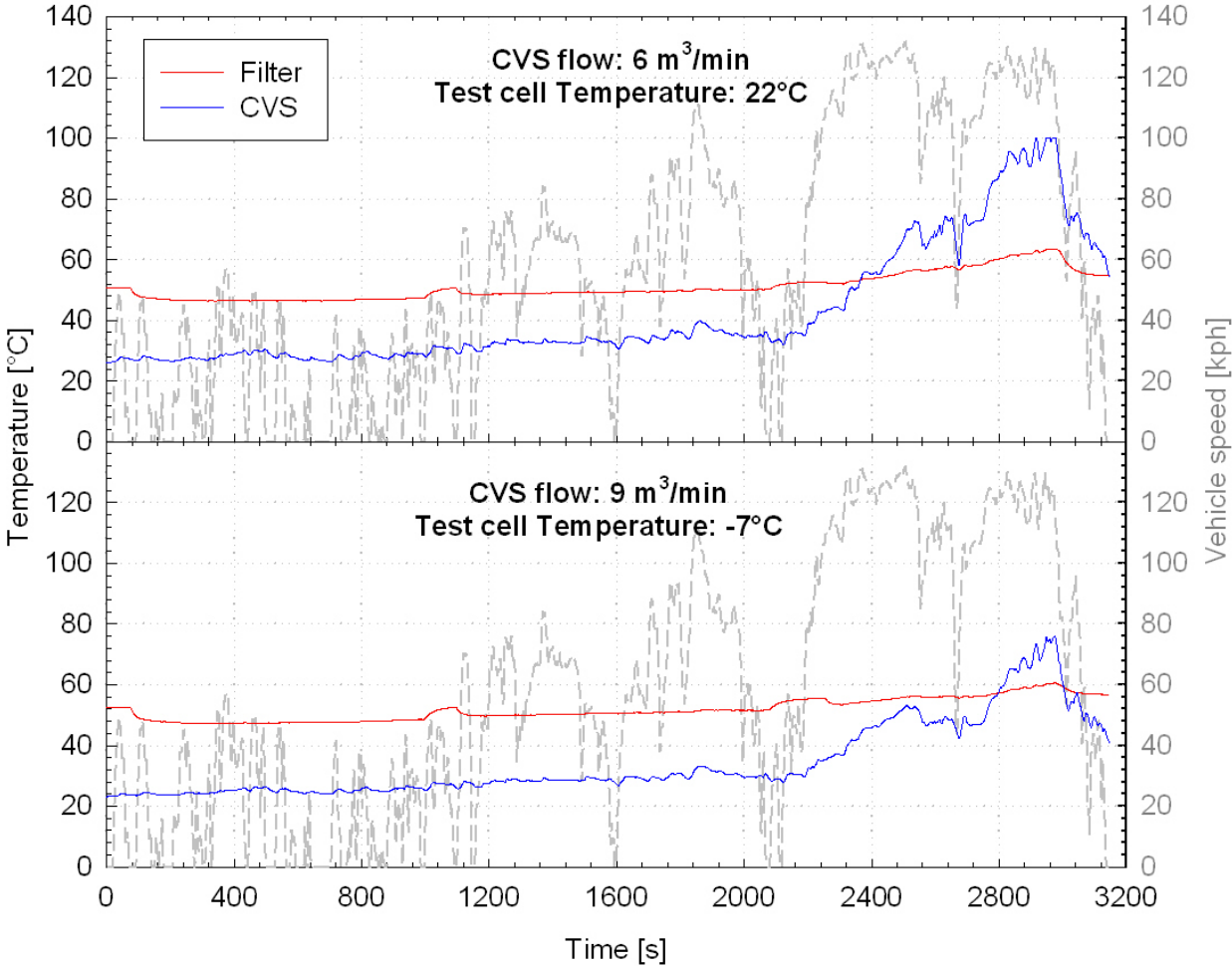


Figure 7: CVS and PM filter face temperatures during regenerative CADC tests at 22°C (upper panel) and -7°C (lower panel) test cell temperatures.

### 3.2 PM EMISSIONS

Figure 8 summarizes the PM emissions measured over the NEDC and the CADC test cycles. The results are plotted against the mileage accumulated since the last regeneration of the DPF. Focusing on the NEDC results, no clear effect of the DPF fill status can be observed. The PM emissions appear to depend mostly on test cell temperature (Figure 9). Under the regulated temperature of 22°C, the PM emissions averaged at 0.3 ( $\pm 0.1$ ) mg/km (range stands for  $\pm$  one standard deviation). This figure is well below the emission standard of 4.5 mg/km. Tests at -7°C resulted in a fivefold increase in the PM emissions, averaging at 1.5 ( $\pm 0.3$ ) mg/km, while the single test at -2°C yielded a PM emission of 0.7 mg/km.

The CADC tests showed a much lower sensitivity of PM on the test cell temperature. For the tests where no active regeneration took place, the PM emissions averaged at 0.6 ( $\pm 0.3$ ) mg/km. This suggests that the test cell temperature mainly affects the PM emitted over the cold start phase of the NEDC. Unfortunately, it was not possible to verify this since a single TX40 filter was employed over the entire NEDC.

In the CADC tests where the DPF regenerated actively, the PM emissions increased to levels as high as 14 mg/km. Active regeneration occurred approximately every 400 to 500 km for this vehicle. The amount of PM emitted during these tests was found to depend on the mileage accumulated since the last regeneration of the DPF vehicle. This is in line with the intuition that sulphates accumulated in the DPF during normal operation are being released when the DPF regenerates constituting most of the emitted PM. However, there is no information available on the chemistry of the PM samples to support this argument.

Figure 11 summarizes the PM results obtained in the tests where a back-up filter was also employed. Practically the same filter mass was collected on the primary and back-up filter in the NEDC test at 22°C. This suggests gaseous adsorption as the main source of the collected PM. The absolute levels were approximately one order of magnitude higher than background PM, and therefore the PM comes from engine exhaust. High PM mass (~65% of what collected on the primary filter) was also collected on the secondary filter during the CADC test at 22°C, also suggesting high contribution of adsorbed material.

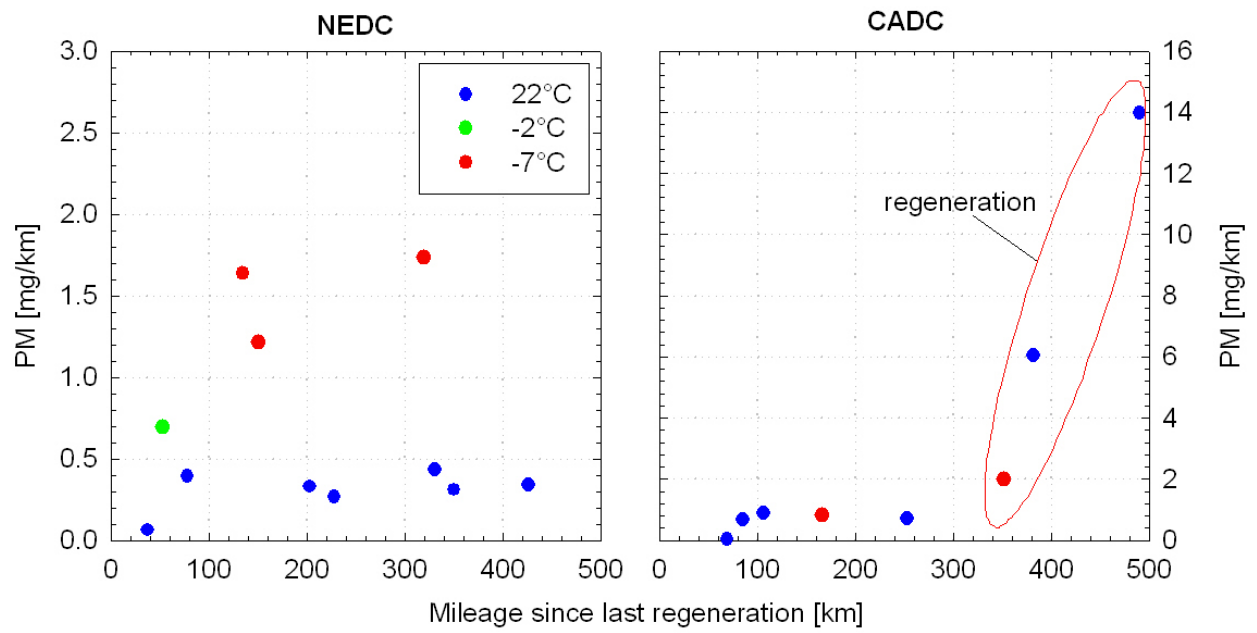


Figure 8: PM emissions over the cold start NEDC (left hand panel) and CADC (right hand panel) tests plotted against the accumulated mileage since last regeneration.

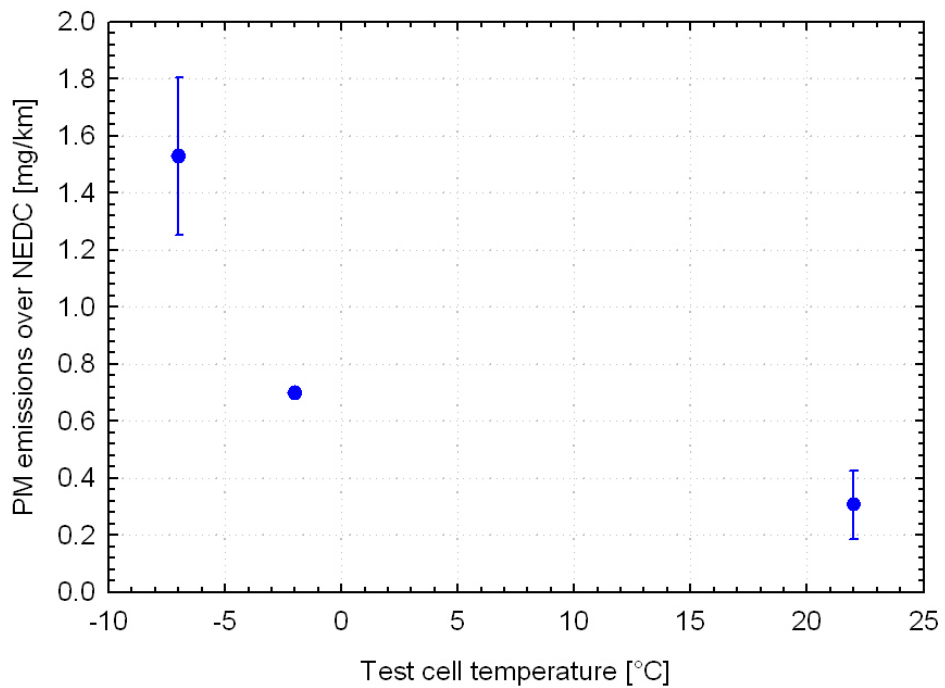


Figure 9: PM emissions over the NEDC at different test cell temperatures. Error bars correspond to  $\pm 1$  standard deviation.



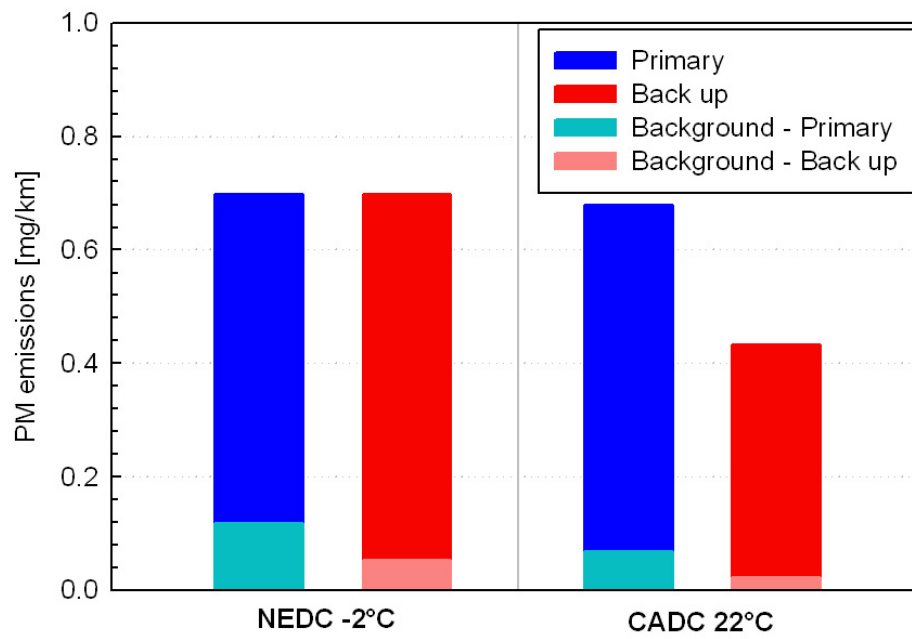


Figure 10: Comparison of the PM emissions determined from the primary and secondary TX40 filters.

### 3.3 PN EMISSIONS

#### 3.3.1 Real time traces

Figure 11 shows some representative traces of “non-volatile” particle number emission rates, as defined in the regulations, for cold start NEDC tests at 22°C. The particle number emissions are found to follow the exhaust flowrate traces, also shown in the graph, over the entire duration of the cycle. A cold start effect can also be identified, resulting in three times higher emissions over the first ECE15 elementary cycle. Such emission performance is different from that of the golden, Euro 4 technology, vehicle tested in the frame of the PMP Light Duty Interlaboratory Correlation Exercise [1, 2]. The particle emissions of the latter were found to occur almost entirely over the cold start phase of the NEDC, following which they dropped to near-zero levels.

The behaviour of the vehicle tested in the present study is indicative of a higher porosity DPF system. The filtration efficiency of the DPF, however, was sufficient high to bring the cycle average particle number emissions below  $2 \times 10^{11}$  #/km, i.e. three times below the Euro 6 threshold, over all NEDC tests performed. The filtration efficiency improved as soot started accumulating in the DPF, with the emissions exhibiting an almost three-fold decrease after approximately 300 km mileage accumulation.

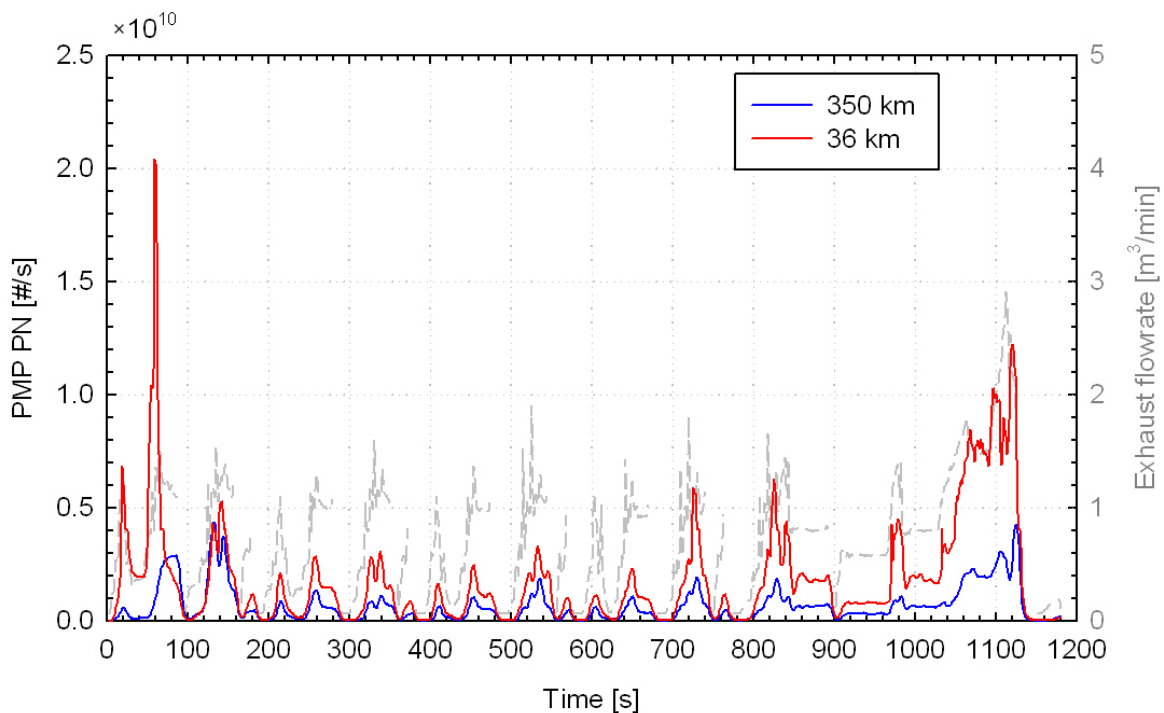


Figure 11: “Non-volatile” particle number emission rates over cold start NEDC at 22°C test cell temperatures for relatively clean (red curve – 36 km mileage accumulated since last regeneration) and loaded (blue curve – 350 km mileage accumulated since last regeneration) DPF.

Figure 12 shows typical particle number emission traces over two CADC tests, where no active regeneration of the DPF took place. Again, the particle emissions were found to follow

the exhaust flowrate trace over the whole duration of the cycle. Again the absolute emission levels were found to strongly depend on the soot loading of the DPF, with the emissions downstream of a relatively clean DPF (approximately 70 km after regeneration) being almost twice as much compared to those after ~200 km of accumulated mileage.

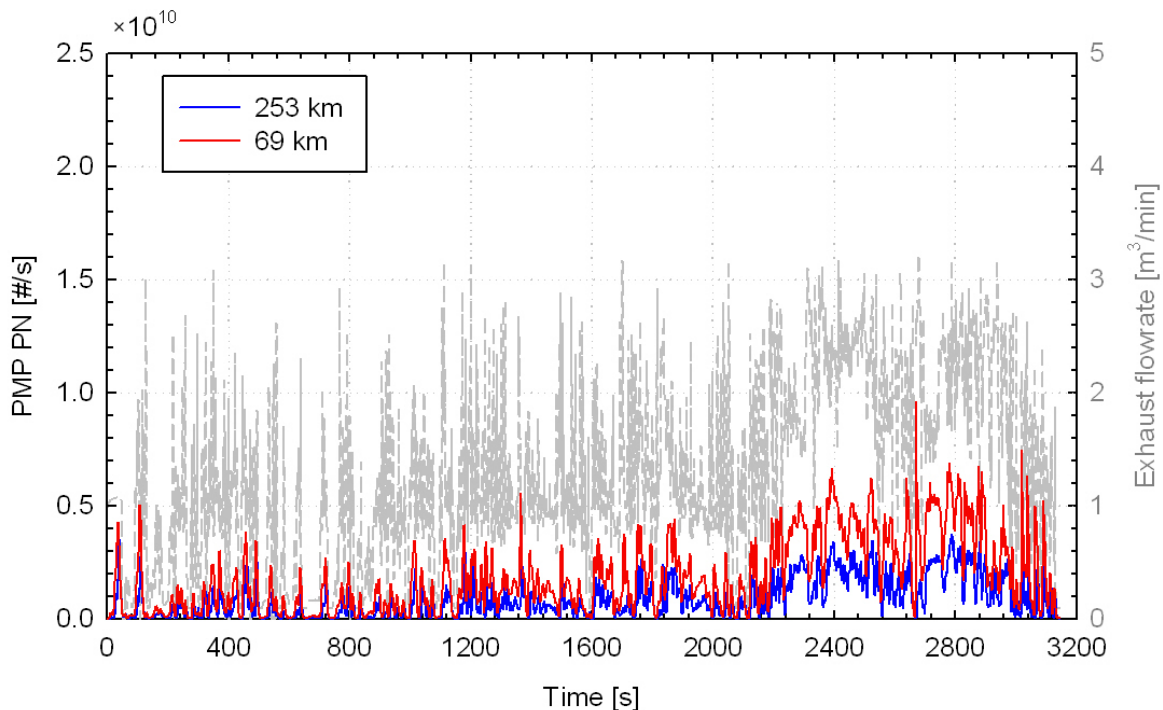


Figure 12: “Non-volatile” particle number emission rates over CADC at 22°C test cell temperatures for relatively clean (red curve – 69 km mileage accumulated since last regeneration) and loaded (blue curve – 253 km mileage accumulated since last regeneration) DPF.

### 3.3.2 Effect of DPF soot load

As already mentioned in the previous section, the particle number emissions were found to strongly depend on the soot load of the DPF. This is shown more clearly in Figure 13, where the cycle average number emissions over the cold start NEDC tests, and the two phases of the cycle, are plotted against the mileage accumulated since the last active regeneration of the DPF. In tests at 22°C, the emissions over the whole NEDC decreased from  $2 \times 10^{11}$  #/km for a clean DPF (36 km accumulated mileage since last active regeneration) to  $5 \times 10^{10}$  #/km after 425 km accumulated mileage. Similar trends were observed over the ECE and EUDC parts of the cycle, with the distance average emissions over the urban part being twice as high compared to those over the extra-urban part. Auxiliary power consumption of up to 600 W did not appear to affect the particle number emissions.

Interestingly, the tests at sub-zero ambient temperatures yielded systematically lower emissions, which furthermore exhibited a smaller dependence on the mileage accumulated after the last DPF regeneration. The particle emissions decreased from  $7 \times 10^{10}$  #/km, 50 km after the last active regeneration of the DPF, to  $4 \times 10^{10}$  #/km after some additional 270 km of operation at sub-ambient test cell temperatures.

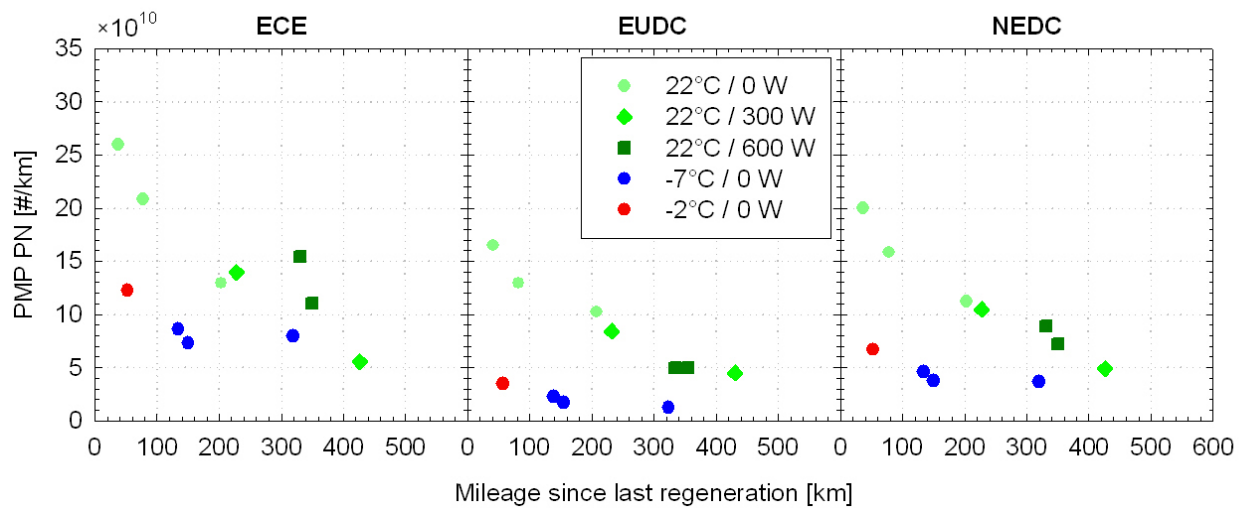


Figure 13: Cycle-average “non-volatile” particle number emissions over the cold start NEDC (right-hand panel) and the ECE (left-hand panel) and EUDC (mid panel) phases of the cycle, plotted against the mileage accumulated since the last active regeneration of the DPF.

The lower particle number emissions at sub-zero ambient temperatures are associated with the lower EGR rates at these conditions. This is evident in Figure 14 comparing the  $\text{NO}_x$  emissions and the EGR valve positioning for cold start NEDCs at test cell temperatures of  $-2^\circ\text{C}$  and  $22^\circ\text{C}$ . Lower EGR rates were employed over the sub-zero temperature tests resulting in 2.5 times higher  $\text{NO}_x$  emissions. Accordingly, the engine out PM levels are expected to decrease owing to the well known  $\text{NO}_x$ -PM tradeoff. The particular two tests were performed with a relatively clean DPF (less than 50 km mileage accumulated since the last active regeneration of the DPF), and therefore similar filtration efficiencies of the DPF were expected. The “non-volatile” particle number emissions downstream the DPF, as measured in the CVS tunnel, were 3 times lower in the test at  $-2^\circ\text{C}$ .

Figure 15 summarizes the particle number emissions over the urban, rural and motorway parts of the non-regenerative CADC tests, plotted against the mileage accumulated since the last active regeneration of the DPF. The trends were similar to those observed over the regulated NEDC test cycle (Figure 13). The distance average emissions over the urban part, decreased from  $1.5 \times 10^{11}$  #/km, 70 km after the last active regeneration of the DPF, to  $7 \times 10^{10}$  #/km after 180 km operation at  $22^\circ\text{C}$  test cell temperatures. Sub-zero temperature operation resulted in more than 2 times lower number emissions. The distance average emissions over the rural and motorway parts of the cycle were on average 44% ( $\pm 5\%$ ) and 26% ( $\pm 20\%$ ), lower compared to those over the urban part of the CADC.

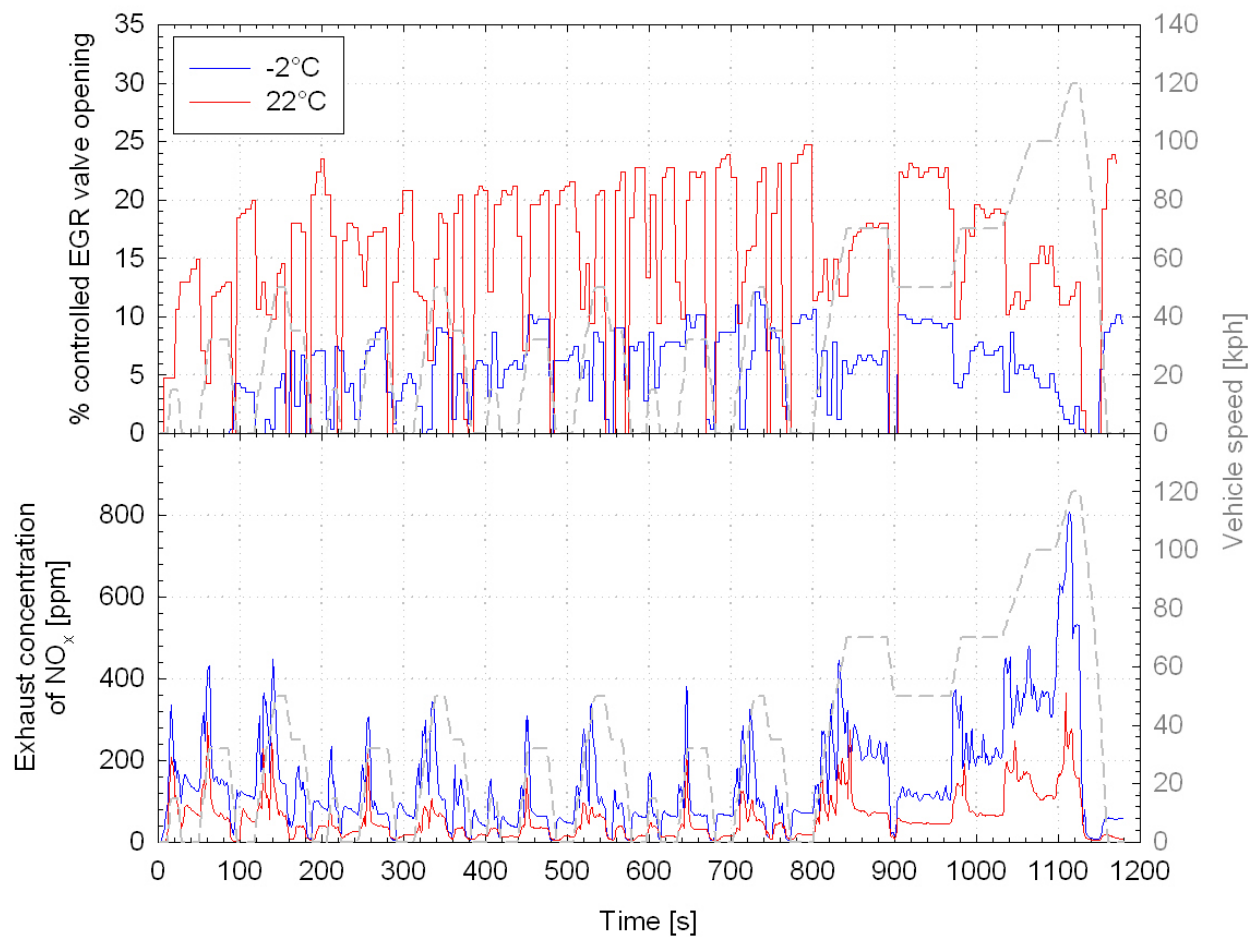


Figure 14: ECU signals on the EGR valve opening (upper panel) and NO<sub>x</sub> concentrations in the exhaust (lower panel) over cold start NEDC at 22°C (blue curves) and -2°C (red curves) test cell temperatures.

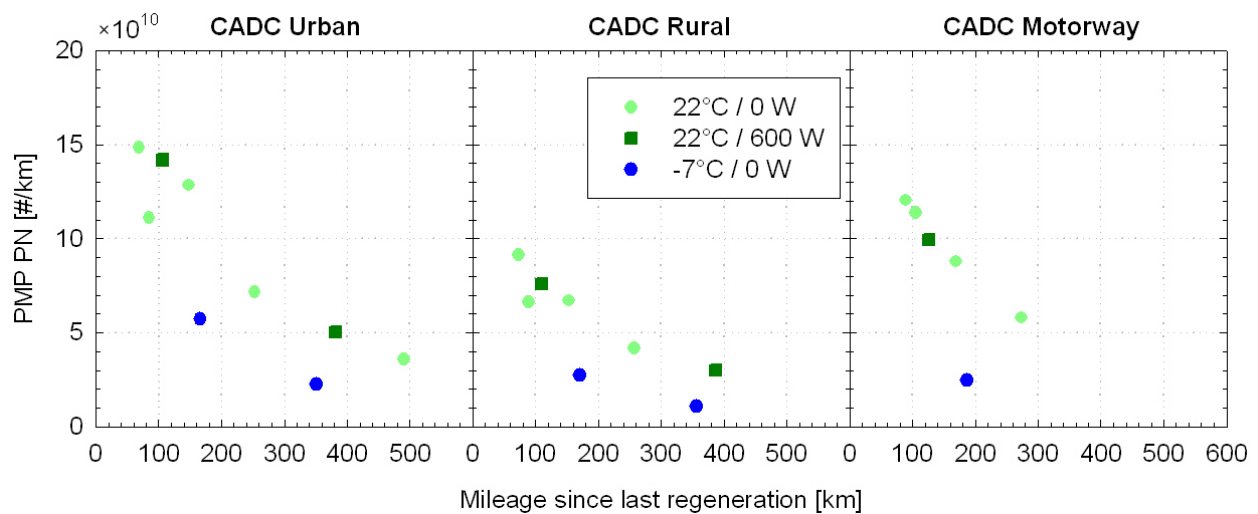


Figure 15: Cycle-average “non-volatile” particle number emissions over the urban (left-hand panel), rural (mid panel) and motorway (right-hand panel) part of the CADC, plotted against the mileage accumulated since the last active regeneration of the DPF.

One particular active regeneration event occurred over the last part of a CADC test cycle and was interrupted before it was completed (lower panel in Figure 5). The particle emissions over the three subsequent conditioning EUDCs, shown in Figure 16, suggested a rapid increase of the filtration efficiency. The distance average emissions decreased from  $26 \times 10^{11}$  #/km over the first EUDC repetition, to  $3 \times 10^{11}$  #/km over the second EUDC and eventually  $0.6 \times 10^{11}$  #/km over the last EUDC. This almost two orders of magnitude decrease in particle number emissions is obviously related to the filtration efficiency improvement brought by the storage of soot inside the DPF wall and subsequently the development of a soot cake inside the DPF. The emission reduction is too high to be associated with the warming up of the engine.

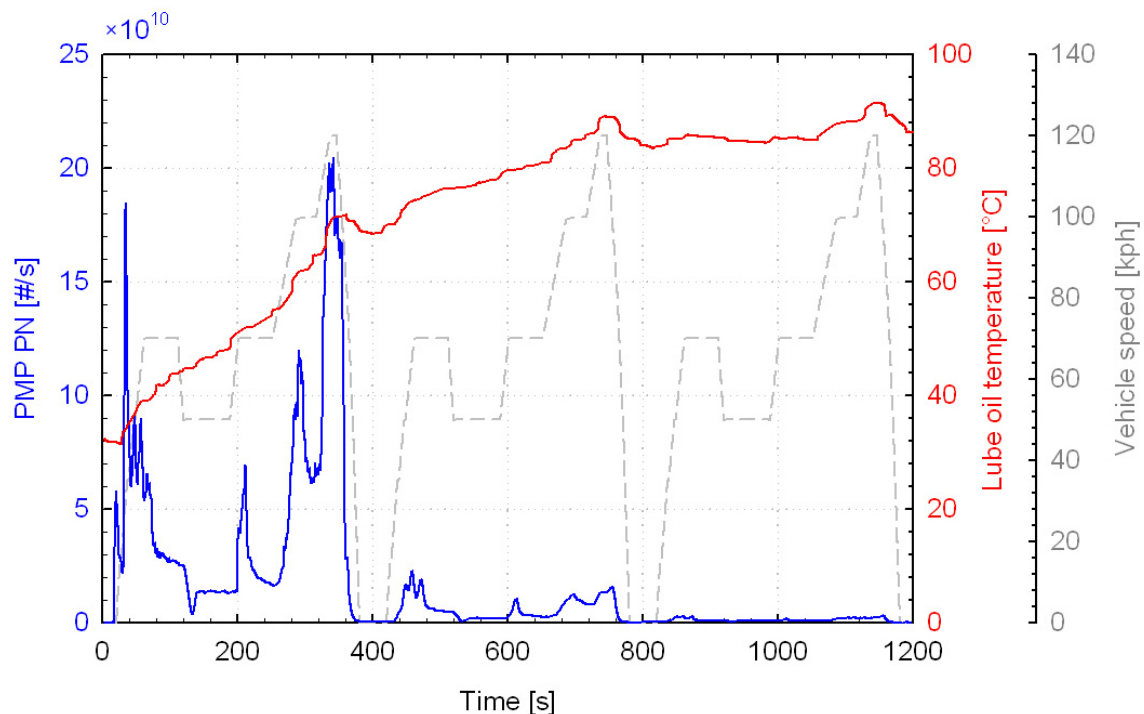


Figure 16: “Non-volatile” particle number emissions over three conditioning EUDCs at  $-7^{\circ}\text{C}$ , commencing immediately after the completion of an active regeneration event.

### 3.3.3 Emissions during regeneration

The DPF regenerated actively four times during the measurement campaign. The first active regeneration event occurred during a free acceleration test performed in some preliminary tests upon installation of the vehicle in the chassis dynamometer. No information on particle number emissions is available for the particular test. The remaining three regeneration events occurred over CADC tests.

The cycle average emissions during these particular CADC tests are compared to those where no regeneration took place in Figure 17. Particle number emissions during regenerative CADCs, increased by at least one order of magnitude from the baseline levels. The emissions during the two regenerative CADC tests at  $22^{\circ}\text{C}$  ambient test cell temperatures were  $17 \times 10^{11}$  #/km and  $19 \times 10^{11}$  #/km. The cycle average particle number emissions for the regenerative CADC test at  $-7^{\circ}\text{C}$  were somehow lower,  $10 \times 10^{11}$  #/km,

mainly because the CADC test finished before the active regeneration was concluded, as it is evident in the lower panel of Figure 5.

It can also be seen from the figure that active regeneration took place in the first CADC test after at least 350 km mileage accumulated on the vehicle. In one series of tests, regeneration occurred after approximately 500 km accumulated on the vehicle. In this particular case, the vehicle was only tested over NEDCs and EUDCs for more than 300 km before the active regeneration event, which started over the rural part of the CADC cycle.

The real time traces of the “non-volatile” particle number emissions, as defined in the regulations, for the three regenerative CADC tests are shown in Figure 18. The regulated particle number emissions were found to increase from a level of less than  $3 \times 10^7$  #/s to above  $3 \times 10^9$  #/s during the active regeneration events, the duration of which being approximately 10 min.

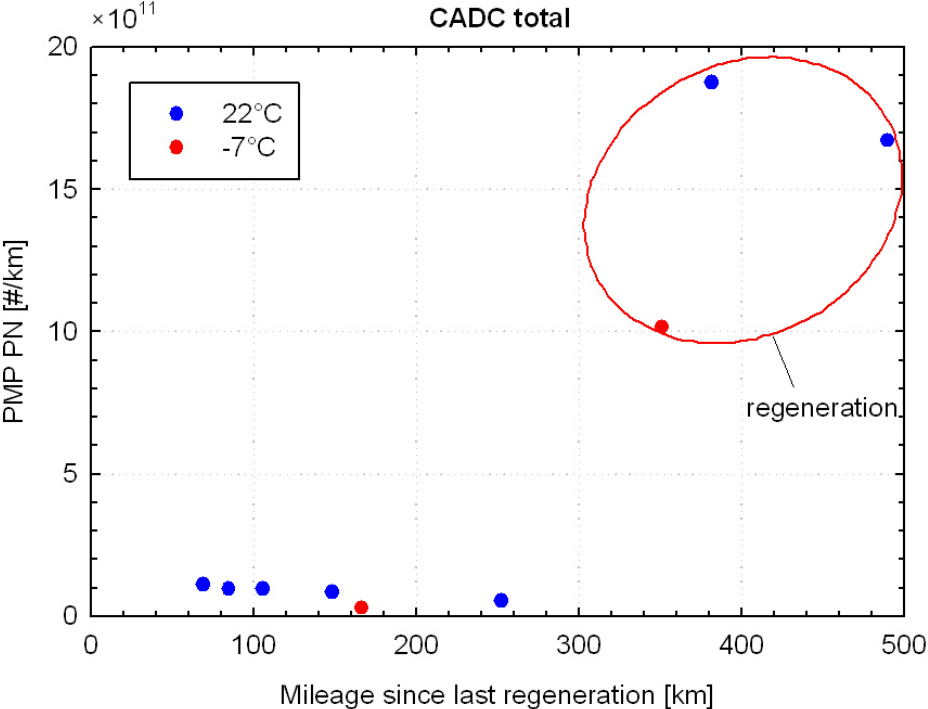


Figure 17: Cycle average “non-volatile” particle number emissions over regenerative and non-regenerative CADC tests.

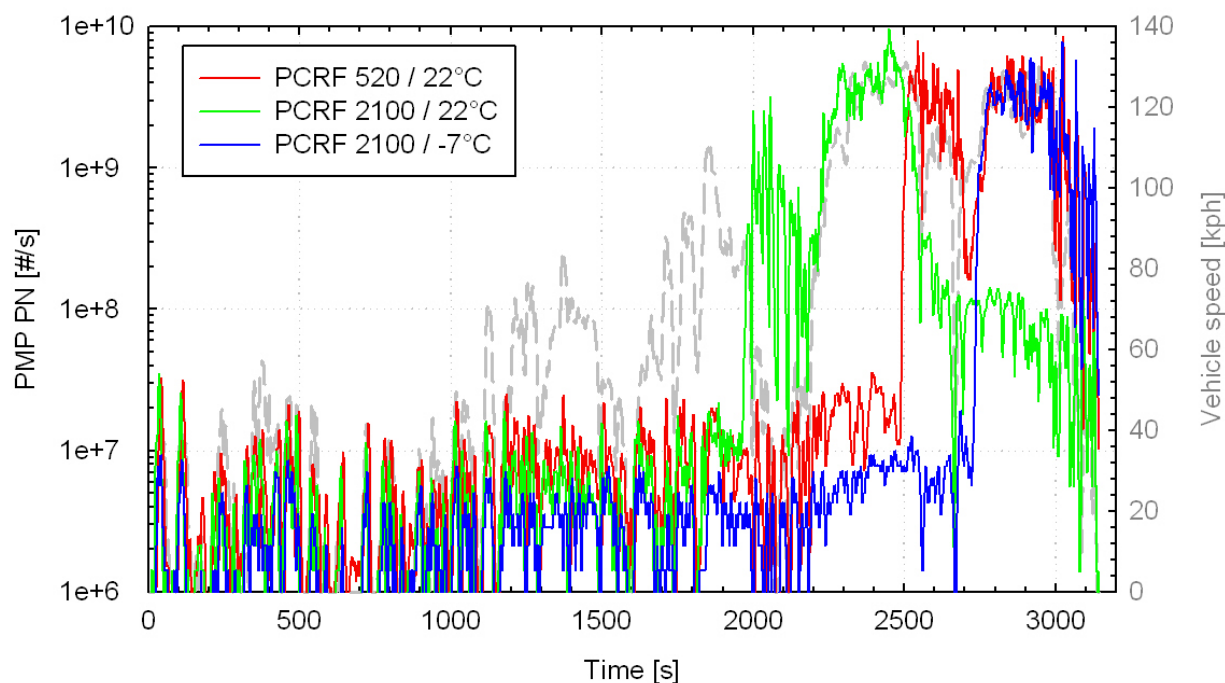


Figure 18: Real time traces of “non-volatile” particle number emissions over the three CADC tests during which the DPF regenerated actively.

### 3.3.4 Sub 23 nm particles

The use of CPCs with 50% detection efficiencies ( $d_{50}$ ) at sub-23 nm sizes, provided some information on the amount of emitted nano-sized “non-volatile” particles that are not considered in the regulations. Figure 19, compares the number emission rates over the different phases of the cold start NEDCs and the CADCs determined with a CPC having a  $d_{50}$  at 10 nm (TSI 3010 - CPC@10nm) to those measured with a CPC with a  $d_{50}$  at 23 nm (TSI 3010D - CPC@23nm). In all hot-start cycles (EUDC and CADC) performed at 22°C, the CPC@10nm yielded 29% ( $\pm 6.5\%$ ) higher number concentrations, with the relative differences no showing any dependence on the soot loading of the DPF. The relative differences did not also depend on the dilution ratio employed and this suggests that these nano-sized particles are “non-volatile” in nature.

Over the cold start ECE, the differences were somehow larger, with the CPC@10nm measuring on average 58% ( $\pm 26\%$ ) higher emissions than the CPC@23nm. Furthermore, a small dependence on the soot loading could be identified, with the difference averaging at 80% ( $\pm 13\%$ ) for the three tests conducted after less than ~200 km of mileage accumulated on the DPF, and at 37% ( $\pm 13\%$ ) for the three tests with a higher soot load on the DPF. Again the PCRf did not affect the correlations, and therefore the relatively higher signal of the CPC@10nm in these tests, reflects higher concentrations of smaller “non-volatile” particles.

The tests at -7°C suggested an even higher relative contribution of unregulated nano-sized particles that appear to be “non-volatile” in nature, given the good agreement between results obtained at PCRf settings of 300 and 2100. This was particularly evident in the ECE tests, where the CPC@10nm yielded 4 to 5.5 times higher concentrations than the CPC@23nm. Over hot start cycles, the correlation appeared to depend on the driving conditions, with the relative difference decreasing from 120%-140% over the urban part of the CADC, to 60-90%



over CADC rural and motorway. The test point at CADC motorway where no regeneration took place, suggested a difference of 35%.

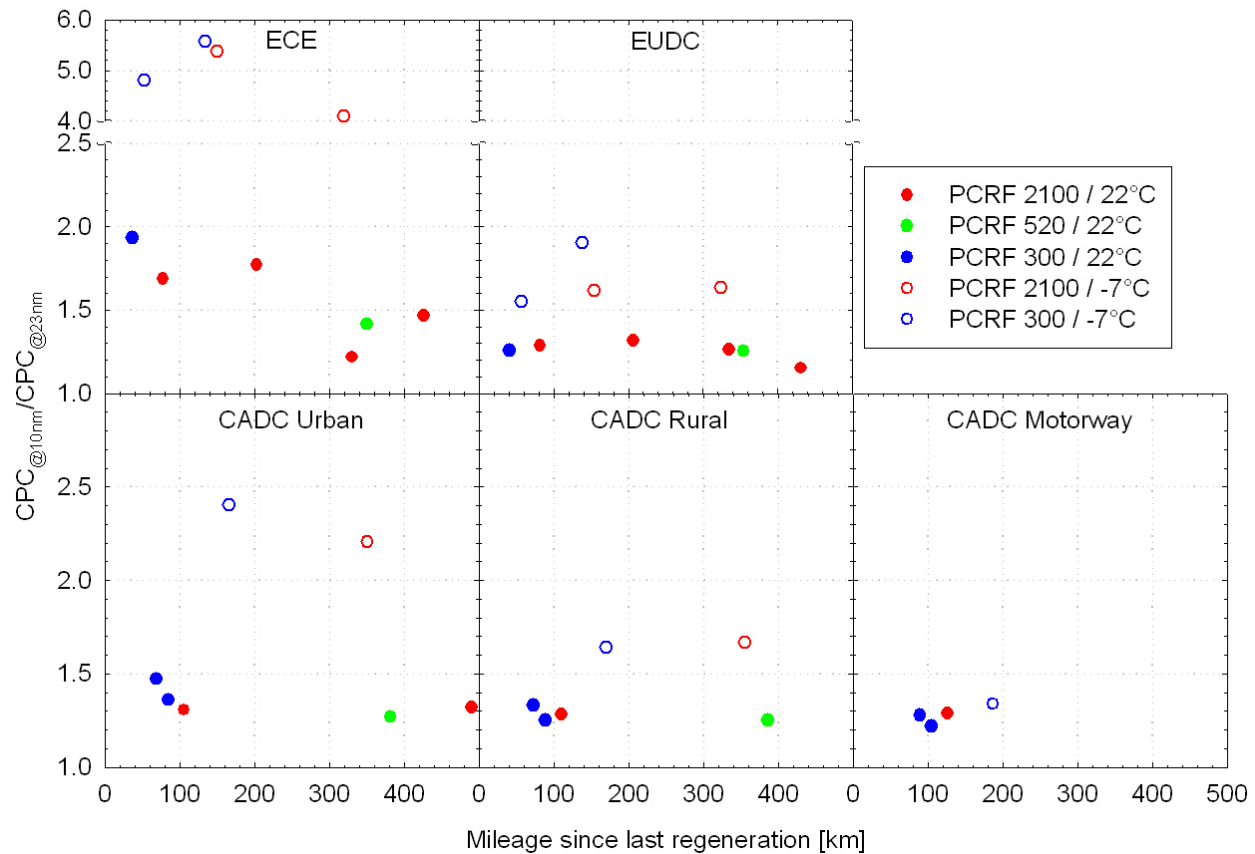


Figure 19: Comparison of the number concentrations of “non-volatile” particles over the ECE and EUDC part of cold start NEDC tests (upper panels) and the three phases of the CADC (lower panels), measured with two CPCs having nominal 50% detection efficiencies at 10 nm and 23 nm.

Similar trends are observed when comparing the responses of the  $CPC_{@4.5nm}$  to those of the  $CPC_{@23nm}$  (Figure 20). Over hot start tests at 22°C, the  $CPC_{@4.5nm}$  measured on average 64% ( $\pm 18\%$ ) higher distance-average emissions from the  $CPC_{@23nm}$ , with the relative difference showing no obvious dependence on the dilution ratio employed. Over the cold start ECE at 22°C, the relative difference appeared to be higher for low DPF soot loading, averaging at 148% ( $\pm 22\%$ ).

Over cold-start ECE tests at -7°C, the relative differences ranged between 450% and 800%. Tests at -7°C with the engine hot resulted in lower differences, which again depended on the driving conditions. The relative differences decreased from 280%-320% over CADC urban to 110%-170% over CADC rural and EUDC and 70% over the non-regenerative CADC motorway.

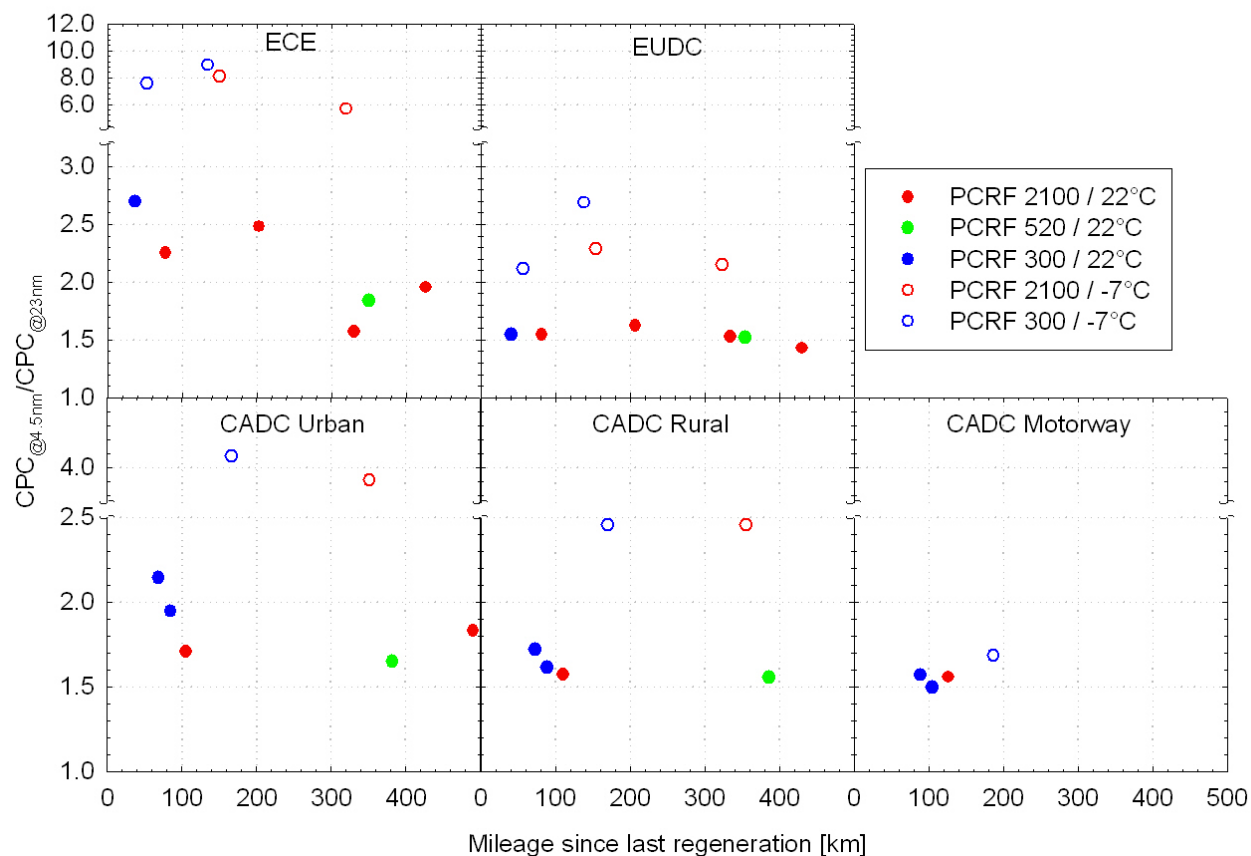


Figure 20: Comparison of the number concentrations of “non-volatile” particles over the ECE and EUDC part of cold start NEDC tests (upper panels) and the three phases of the CADC (lower panels), measured with two CPCs having nominal 50% detection efficiencies at 4.5 nm and 23 nm.

Figure 21 compares the real time responses of the different CPCs over cold start NEDCs at  $-7^{\circ}\text{C}$  and  $22^{\circ}\text{C}$ . At  $22^{\circ}\text{C}$  ambient temperature, similar traces were observed from all CPCs. The contribution of sub-23 nm particles decreased over time, as the engine warmed up, with the difference between the indications of the  $\text{CPC}_{@10\text{nm}}$  and  $\text{CPC}_{@23\text{nm}}$  decreasing from 83% over the first ECE15 to 42% over the fourth ECE15 and 29% over the EUDC part of the cycle. The corresponding figures for the differences between the indications of the  $\text{CPC}_{@4.5\text{nm}}$  and the  $\text{CPC}_{@23\text{nm}}$  were 149%, 79% and 55%, respectively.

During the tests at  $-7^{\circ}\text{C}$ , with similar soot loadings in the DPF, the real time traces of the  $\text{CPC}_{@23\text{nm}}$  were found to be systematically lower from those at  $22^{\circ}\text{C}$ , over the entire duration of the cycle. The traces of the CPCs having a  $d_{50}$  at 10 nm and 4.5 nm were distinctly different from those of the  $\text{CPC}_{@23\text{nm}}$ , over the ECE and the first 60 s of the EUDC part. The absolute levels were found to be even higher from those at  $22^{\circ}\text{C}$  over the ECE, but gradually decreased over time, with the difference from the  $\text{CPC}_{@23\text{nm}}$  approaching a value of 50% for the  $\text{CPC}_{@10\text{nm}}$  and 90% for the  $\text{CPC}_{@4.5\text{nm}}$  over the last phase of the EUDC.

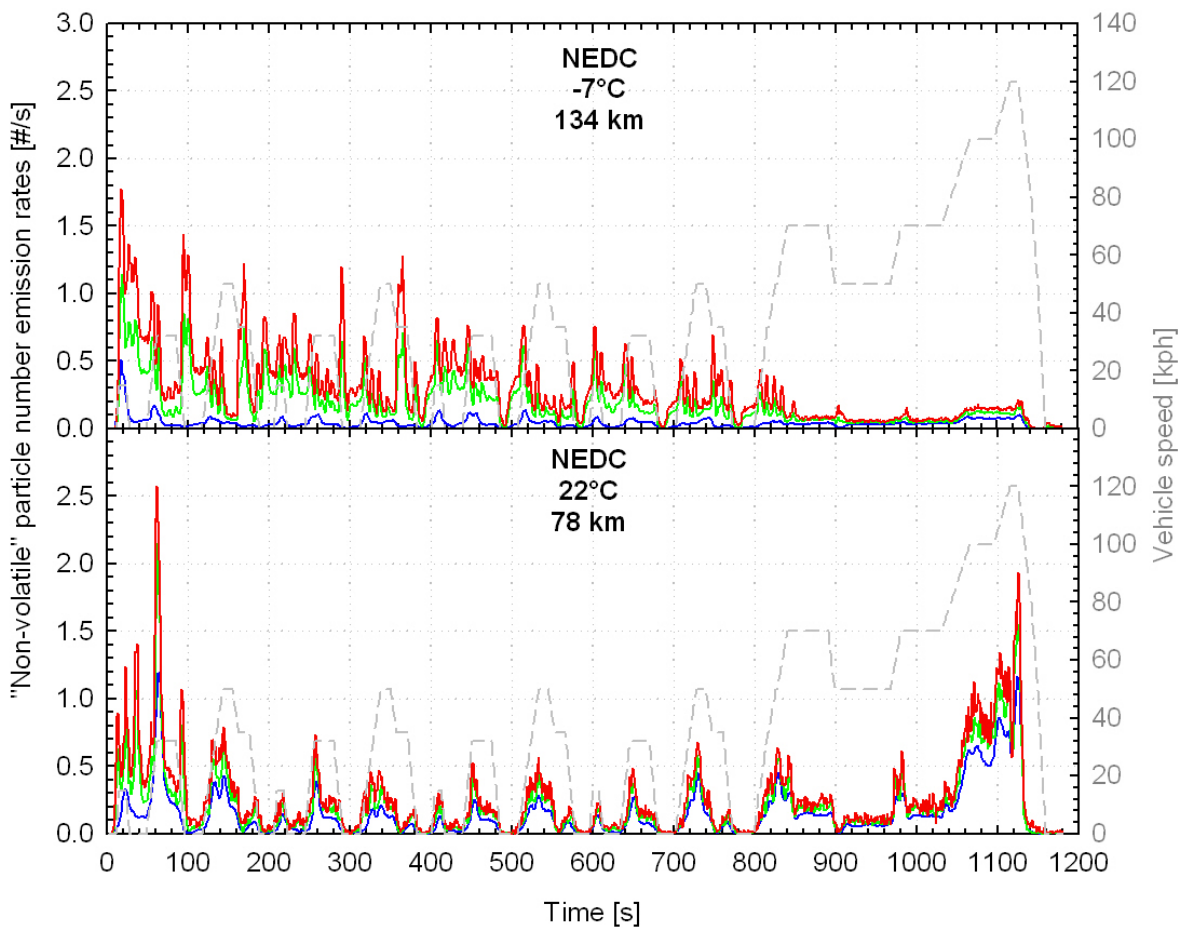


Figure 21: Comparison of real time particle number traces over cold start NEDC at  $-7^{\circ}\text{C}$  (upper panel) and  $22^{\circ}\text{C}$  (lower panel) measured downstream the PMP system with three CPCs having 50% detection efficiencies at 23 nm (blue lines), 10 nm (green lines) and 4.5 nm (red lines).

Increased emissions of sub-23 nm particles were also observed during active regeneration of the DPF system. However, under these conditions, very high emissions of volatile nanoparticles are also observed. During all the active regeneration events, the concentrations measured by the  $\text{CPC}_{@3.5\text{nm}}$  sampling untreated aerosol from the CVS tunnel, increased by more than three orders of magnitude. It was not possible to quantify the absolute levels as the particular CPC got saturated, and remained saturated even several minutes after the completion of the regeneration. Such high concentrations of volatile material necessitate much higher volatile removal efficiencies from the 99% requirement set in the regulations. This is especially true if a CPC with a low cut-off size is employed, given that most of the emitted volatile particles are found to be in the sub-23 nm size range [11].

Figure 22 compares the cycle average emissions over all three phases of the CADC measured with the three CPCs sampling downstream the PMP system for all three tests where regeneration took place. In the two tests at  $22^{\circ}\text{C}$ , similar levels ( $2.9$  to  $3.5 \times 10^{12}$  #/km) were recorded with the  $\text{CPC}_{@23\text{nm}}$  even if the dilution ratio differed by almost 4 times. The test at  $-7^{\circ}\text{C}$  resulted in about 40% lower emissions but during this particular test, the regeneration event was interrupted. Interestingly, the emission levels determined with CPCs having a  $d_{50}$  below 23 nm appeared to depend on the PCRf value employed. In the two tests performed at a PCRf value of 2100, the  $\text{CPC}_{@10\text{nm}}$  yielded similar levels to those of the  $\text{CPC}_{@23\text{nm}}$ ,

when at the same time the  $CPC_{@4.5nm}$  measured 2.4 to 4.1 times higher emissions. It should be noted here that the maximum concentrations measured with the 3010 CPCs ( $CPC_{@23nm}$  &  $CPC_{@10nm}$ ) were lower than  $4000 \text{ \#/cm}^3$  and therefore uncertainties in the coincidence correction employed should not affect the accuracy of these measurements. The good agreement between the  $CPC_{@23nm}$  and the  $CPC_{@10nm}$ , measuring at least 2.4 times lower concentrations from the  $CPC_{@4.5nm}$ , suggests the presence of a nucleation mode peaking below the lower detectable size of these CPCs.

A comparison of the regenerative CADC tests at  $22^\circ\text{C}$ , suggests that a fourfold increase in the dilution ratio increases the contribution of sub-23 nm particles from 0% ( $CPC_{@10nm}$ ) and 140% ( $CPC_{@4.5nm}$ ) to 43% and 420%, respectively. This is an indication that these sub-23 nm particles are volatile in nature, either surviving evaporation or re-nucleating downstream of the ET.

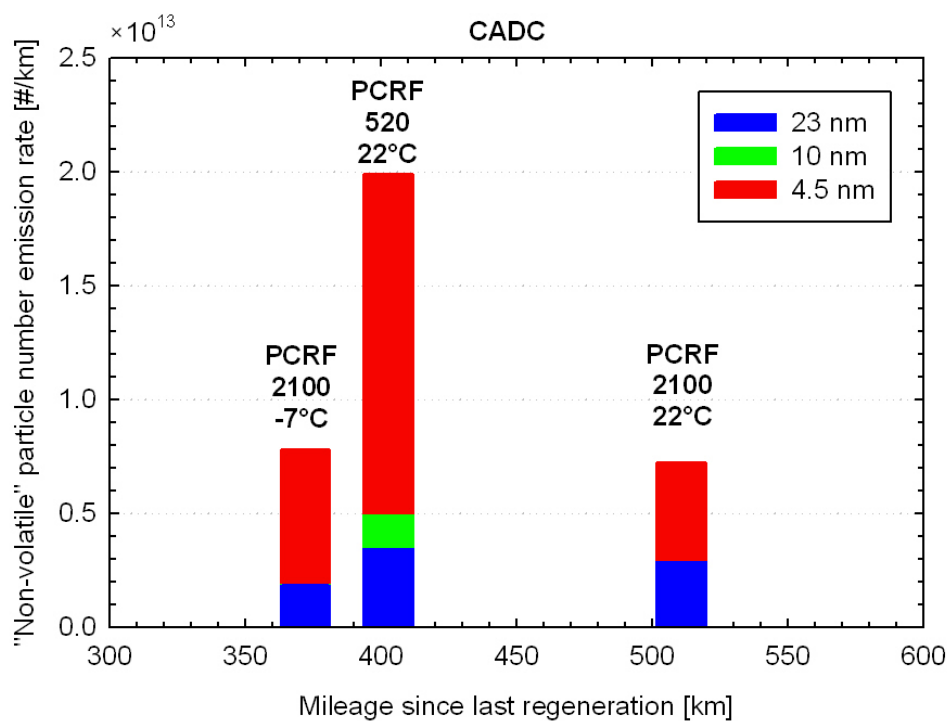


Figure 22: Cycle average emissions of "non-volatile" particles measured with three CPCs of  $d_{50}$  at 23 nm, 10 nm and 4.5 nm, over CADC tests where active regeneration took place.

## 4 CONCLUSIONS

The particle emissions of a Euro 5 technology, DPF-equipped diesel passenger car were investigated in the present study. The vehicle was tested under NEDC and CADC test cycle at both 22°C and -7°C test cell temperatures. The aerosol properties examined included PM mass and “non-volatile” particle numbers using three CPCs with 50% counting efficiencies at 23 nm (regulated), 10 nm and 4.5 nm.

PM emissions over the NEDC cycle were found to depend strongly on the test cell temperature, with tests at -7°C yielding on average 5 times higher particulate mass (~1.5 mg/km) compared to those under the legislated 22°C. When a back-up filter was employed however, similar levels of mass were collected on both filters, suggesting adsorbed material as the main contributor to PM. The test cell temperature did not affect the PM emissions over the CADC, which averaged at 0.6 mg/km for the tests where the DPF did not regenerate actively. This indicates that the observed test cell temperature dependence of the PM emissions over NEDC is associated with the cold start operation of the vehicle. When the DPF regenerated actively over the Motorway part of the CADC, the PM emissions were found to increase up to 14 mg/km. The PM emissions during these tests were found to increase with the mileage accumulated on the vehicle since the last regeneration of the DPF. This behaviour points towards release of material (presumably sulphates) collected in the DPF that is subsequently released during regeneration. However, no information is available on the chemistry of the PM to verify this assumption.

The regulated PMP particle number measurement procedure was found to be sensitive enough to identify the increase in the filtration efficiency as soot accumulates inside the DPF. In contrast to the PM results, vehicle driving at -7°C resulted in approximately two times lower particle number emissions. This was found to be related to the operation of the engine at lower EGR rates resulting in lower engine out particle number emissions. High number concentrations of “non-volatile” particles were observed during active regeneration of the DPF, with the cycle average emissions over CADC increasing by more than one order of magnitude. The average emissions over non-regenerative CADC tests were around  $9 \times 10^{10}$  #/km while the two CADC tests at which the DPF regenerated actively averaged at  $170 \times 10^{10}$  #/km. The DPF was found to regenerate over the first CADC test occurring after 350 km accumulated mileage, or equivalently once every 8 CADC tests (50 km mileage each). The weighted average emissions over the 8 CADC tests would therefore be  $29 \times 10^{10}$  #/km, still below the limit of  $60 \times 10^{10}$  #/km.

The CPCs having a 50% counting efficiency below 23 nm, yielded systematically higher emissions, with the relative difference depending on the test cycle and the test cell temperature. The CPC having a  $d_{50}$  size at 10 nm yielded about 30% higher concentrations in hot-start tests at 22°C ambient temperature. During these tests the CPC with a  $d_{50}$  size at 4.5 nm yielded 65% higher concentrations from the  $CPC_{@23nm}$ . Similar differences were observed when employing different PCRF values, and therefore the nano-sized particles detected are “non-volatile” in nature. Cold start operation, especially at sub-zero ambient temperatures, resulted in elevated concentrations of sub-23 nm particles. In that respect, the CPC with a  $d_{50}$  size at 4.5 nm yielded up to 800% higher emissions from that with a  $d_{50}$  at 23 nm over the cold start ECE tests at -7°C. Still the absolute levels were quite low ( $77 \times 10^{10}$  #/km), being slightly above the legislated limit for particles larger than 23 nm.

During the CADC tests, where active regeneration of the DPF took place, a more than three orders of magnitude increase of volatile nucleation mode particles occurred. High concentrations were also measured downstream of the PMP system with the CPC having a

$d_{50}$  size at 4.5 nm. This is indicative of a nucleation mode peaking at a size below the lowest detectable size (~5 nm) of the CPC having a  $d_{50}$  size at 10 nm. The concentration of this nucleation mode decreased with increasing dilution ratio. This suggests that these nanoparticles are either volatile material surviving evaporation in the ET or an artefact resulting from pyrolysis of volatile material inside the ET [13], both phenomena being suppressed with decreasing the particle concentration entering the ET. The data did not show any evidence of volatile interference in a PMP system with a CPC having a  $d_{50}$  size at 23 nm.

## 5 LIST OF SPECIAL TERMS AND ABBREVIATIONS

CADC	Common Artemis Driving Cycle
CO	Carbon Monoxide
CO <sub>2</sub>	Carbon Dioxide
CPC	Condensation Particle Counter
CVS	Constant Volume Sampler
DOC	Diesel Oxidation Catalyst
DPF	Diesel Particulate Filter
ECE	Urban Part of NEDC
ECS	Emissions Control System
ECU	Electronic Control Unit
EGR	Exhaust Gas Recirculation
ET	Evaporation Tube
EUDC	Extra-urban Part of NEDC
HC	Hydrocarbons
JRC	Joint Research Centre
NEDC	New European Driving Cycle
NO <sub>2</sub>	Nitrogen Dioxide
NO <sub>x</sub>	Nitrogen Oxides
O <sub>2</sub>	Oxygen
PCRF	Particle Concentration Reduction Factor
PM	Particulate Matter
PMP	Particle Measurement Programme
PN	Particle Number
VELA	Vehicle Emissions Laboratory

## 6 REFERENCES

---

- 1 Giechaskiel, B.; Munoz-Bueno, R.; Rubino, L.; Manfredi, U.; Dilara, P.; De Santi, G. and Andersson J. (2007). Particle Measurement Programme (PMP): Particle Size and Number Emissions Before, During and After Regeneration Events of a Euro 4 DPF Equipped Light Duty Diesel Vehicle. SAE Technical Paper 2007-01-1944.
- 2 Anderson, J.; Giechaskiel, B.; Muñoz-Bueno, R.; Sandbach, E. And Dilara, P. (2007). Particle Measurement Programme (PMP) Light-Duty Inter-Laboratory Correlation Exercise (ILCE\_LD) Final Report. EUR 22775 EN.
- 3 Mohr, M.; Forss, A. and Lehmann, U. (2006). Particle Emissions from Diesel Passenger Cars Equipped with a Particle Trap in Comparison to Other Technologies. *Environmental Science and Technology*, 40: 2375-2383.
- 4 Campbell, B.; Peckham, M.; Symonds, J.; Parkinson, J. and Finch, A. (2006). Transient Gaseous and Particulate Emissions Measurements on a Diesel Passenger Car Including DPF regeneration. SAE Technical Paper 2006-01-01079.
- 5 Guo, G.; Xu, N.; Laing, P.M.; Hammerle, R.H. and Maricq, M.M. (2003). Performance of a Catalyzed Diesel Particulate Filter System During Soot Accumulation and Regeneration. SAE Technical Paper 2003-01-0047.
- 6 Mathis, U.; Mohr, M. and Forss A.-M. (2005). Comprehensive Particle Characterization of Modern Gasoline and Diesel Passenger Cars at Low Ambient Temperatures. *Atmospheric Environment*, 39: 107-117.
- 7 Dwyer, H.; Ayala, A.; Zhang, S.; Collins, J.; Huai, T.; Herner, J. and Chau, W. (2010). Emissions from a Diesel Car During Regeneration of an Active Diesel Particulate Filter. *Journal of Aerosol Science*, 41: 541-552.
- 8 Bergmann, M.; Kirchner, U.; Vogt, R. and Benter, T. (2009). On-road and Laboratory Investigation of Low-Level PM emissions of a Modern Diesel Particulate Filter Equipped Diesel Passenger Car. *Atmospheric Environment*, 43: 1908-1916.
- 9 Bikas, G. and Zervas, E. (2007). Regulated and Non-Regulated Pollutants Emitted During the Regeneration of a Diesel Particulate Filter. *Energy and Fuels*, 21:1543-1547.
- 10 Anderson, J. (2006). Final Report of a Test Programme for DFT: Fuel and Lubricant Effects on Particle Emissions from DPF Equipped Diesel Vehicles. Ricardo Report RD 06/240701.2
- 11 Mamakos, A. and Martini, G. (2011). Particle Number Emissions During Regeneration of DPF-equipped Light Duty Diesel Vehicles. A Literature Survey. JRC report, EU 24853 EN.
- 12 United Nations, Economic Commission for Europe, Regulation No 83, Revision 4, "Uniform Provisions Concerning the Approval of Vehicles with Regard to the Emission of Pollutants According to Engine Fuel Requirements", 2011
- 13 Swanson, J. and Kittelson D. (2010). Evaluation of Thermal Denuder and Catalytic Stripper Methods for Solid Particle Measurements. *Journal of Aerosol Science*, 41:1113-1122.
- 14 Directive 2009/30/EC of the European Parliament and of the Council of 23 April 2009 Amending Directive 98/70/EC as Regards the Specification of Petrol, diesel and gas-oil and introducing a mechanism to monitor and reduce greenhouse gas emissions and amending Council Directive 1999/32/EC as regards the specification of fuel used by inland waterway vessels and repealing Directive 93/12/EEC
- 15 André M. (2004). The ARTEMIS European Driving Cycles for Measuring Car Pollutant Emissions. *Science of the Total Environment*, 334-335:73-84.
- 16 Hueglin C., Scherrer L., Burtcher H., "An accurate continuously adjustable dilution system (1:10 to 1:104) for submicron aerosols", *Journal of Aerosol Science* 28 (6), pp. 1049-1055, 1997



---

17 Kasper M., "The number concentration of non-volatile particles – design study for an instrument according to the PMP recommendations", SAE Paper 2004-01-0960, 2004

18 Ntziachristos L., Giechaskiel B., Pistikopoulos P., Samaras Z., "Comparative assessment of two different sampling systems for particle emission type-approval measurements", SAE Paper 2005-01-0198, 2005

European Commission

**EUR 24855 EN – Joint Research Centre – Institute for Energy**

Title: Particle Emissions from a Euro 5a Certified Diesel Passenger Car

Author(s): A. Mamakos, C. Dardiotis, A. Marotta, G. Martini, U. Manfredi, R. Colombo, M. Sculati, P. Le Lijour, G. Lanappe

Luxembourg: Publications Office of the European Union

2011 – 34 pp. – 21 x 29.7 cm

EUR – Scientific and Technical Research series – ISSN 1831-9424

ISBN 978-92-79-20486-9

doi:10.2788/3173

**Abstract**

The particle emissions of a Euro 5 technology DPF-equipped diesel passenger car were characterized under regulated and unregulated conditions. More specifically, the vehicle was tested under the New European Driving Cycle but also under the Common Artemis Driving Cycles. Measurements were conducted at 22°C and -7°C test cell temperatures. The particle characteristics investigated included PM mass emissions as well as “non-volatile” particle number emissions. The PMP compliant particle number measurement system was supplemented with two additional CPCs allowing for the quantification of unregulated sub-23 nm particles in the size bins of 4.5 to 10 nm and 10 nm to 23 nm. The DPF regenerated actively thrice during the measurement campaign providing some information on the emission performance of the vehicle under these conditions.

## **How to obtain EU publications**

Our priced publications are available from EU Bookshop (<http://bookshop.europa.eu>), where you can place an order with the sales agent of your choice.

The Publications Office has a worldwide network of sales agents. You can obtain their contact details by sending a fax to (352) 29 29-42758.

The mission of the JRC is to provide customer-driven scientific and technical support for the conception, development, implementation and monitoring of EU policies. As a service of the European Commission, the JRC functions as a reference centre of science and technology for the Union. Close to the policy-making process, it serves the common interest of the Member States, while being independent of special interests, whether private or national.

LB-NA-24-855-EN-N

